Control Engineering Practice 20 (2012) 1337–1352

Contents lists available at SciVerse ScienceDirect

Control Engineering Practice

journal homepage: www.elsevier.com/locate/conengprac

Adaptive unified motion control of mobile manipulators

Víctor Andaluz [a,*], Flavio Roberti [b,c], Juan Marcos Toibero [b,c], Ricardo Carelli [b,c]

[a] Facultad de Informática y Electrónica, Escuela Superior Politécnica de Chimborazo, Panamericana Sur km 1 1/2, Riobamba, Ecuador
[b] Instituto de Automática, Universidad Nacional de San Juan, Av. San Martin Oeste 1109, San Juan, Argentina
[c] Concejo Nacional de Investigaciones Científicas y Técnicas, Argentina

ARTICLE INFO

Article history:
Received 8 February 2011
Accepted 30 July 2012
Available online 30 August 2012

Keywords:
Mobile manipulator
Unified motion control
Non-linear systems
Adaptive control
Stability proof

ABSTRACT

This paper presents a unified motion controller for mobile manipulators which not only solves the problems of point stabilization and trajectory tracking but also the path following problem. The control problem is solved based on the kinematic model of the robot. Then, a dynamic compensation is considered based on a dynamic model with inputs being the reference velocities to the mobile platform and the manipulator joints. An adaptive controller for on-line updating the robot dynamics is also proposed. Stability and robustness of the complete control system are proved through the Lyapunov method. The performance of the proposed controller is shown through real experiments.

1. Introduction

Mobile manipulator is nowadays a widespread term that refers to robots built with a robotic arm mounted on a mobile platform. This kind of system, which is usually characterized by a high degree of redundancy, combines the manipulability of a fixed-base manipulator with the mobility of a wheeled platform. Such systems allow the most usual missions of robotic systems which require both *locomotion* and *manipulation* abilities. They are useful in multiple applications in different industrial and productive fields, such as mining, construction, rescue missions or for people assistance (Das, Russell, Kircanski, & Goldenberg, 1999; Khatib, 1999). In recent years, much effort has been done to develop strategies for solving the motion problem of mobile manipulators. In most cases, the proposed controllers focus on only one of the motion problems: point stabilization (Gilioli & Melchiorri, 2002; Tsakiris, Kapellos, Samson, Rives, & Borrelly, 1997), path following (Chuyan, Zhang, & Sun, 2006; Egerstedt & Hu, 2000; Mazur & Szakiel, 2009), or trajectory tracking (Chi-wu & Ke-fei, 2009; Dong, 2002; White & Bhatt, 2009; Xu, Zhao, Yi, & Tan, 2009). At the very least, the proposed controllers address two motion problems (Monastero & Fiorini, 2009), but to the best of our knowledge, no control schemes have been reported to solve all the three above mentioned motion objectives. The control schemes can be classified into two categories. The first one is based on a decentralized control law, which uses a controller for the mobile platform and another one for the manipulator arm. The second category employs a single control law for the entire mobile manipulator system.

Regarding the point stabilization problem (Tsakiris et al., 1997) proposed a visual servoing technique to address the point stabilization problem. The proposal uses only the visual information provided by a camera mounted on the end-effector of the robotic arm. Another visual servoing technique is proposed in Gilioli and Melchiorri (2002) for solving the point stabilization problem. Here, the arm's joint displacements information is combined with the visual information in a hybrid control strategy. On the other hand, White and Bhatt (2009) solve the trajectory tracking problem including obstacles, by using an algorithm with two reference torque signals, one for the mobile platform and another for the end-effector of the manipulating arm. Results are illustrated with real experiments. Ge, Ye, Jiang, and Sun (2008) use a sliding mode control to solve the tracking trajectory problem for a mobile manipulator with a four-wheeled mobile platform. Authors propose a control system decomposed into two subsystems: a sliding mode control for the mobile platform and a non-singular terminal sliding mode control for the manipulator. Xu et al. (2009) propose a neural network-based sliding mode controller, which uses a neural network to identify the unstructured system dynamics. The controller is applied to an omnidirectional wheeled mobile manipulator.

As regarding the path following problem, the work in Egerstedt and Hu (2000) presents a platform independent control for mobile manipulation, and a coordinated trajectory following is proposed and analysed. Given a path for the gripper to follow, the idea is to plan another path for the mobile base. The proposed controller is validated by simulation. Chuyan et al. (2006) presents a controller based on a neural-network for dynamic

* Corresponding author. Tel.: +593 3 2998200; fax: +593 3 2317001.
E-mail address: vandaluz@espoch.edu.ec (V. Andaluz).

0967-0661/$ - see front matter © 2012 Elsevier Ltd. All rights reserved.
http://dx.doi.org/10.1016/j.conengprac.2012.07.008

compensation and coordinated control of the mobile manipulator. Recently, Mazur and Szakiel (2009) addressed the path following problem for two types of nonholonomic mobile manipulators. A cascade structure of two controllers is proposed to achieve the motion along the desired path while preserving an appropriate coordination between the mobile platform and the robotic arm.

To reduce performance degradation, on-line parameter adaptation is relevant in applications where the mobile manipulator dynamic parameters may vary, such as load transportation. It is also useful when the knowledge of the dynamic parameters is limited. Some of the most relevant works addressing the motion adaptive control problem of mobile manipulators are now commented. Phuong, Duy, Jeong, Kim, and Kim (2007) presents an adaptive tracking control method for a welding mobile manipulator with a kinematic model in which several dimensional parameters are unknown. The design of the controller is based on the Lyapunov method. Wu, Feng, and Hu (2005) presents the output tracking control problem of a general mobile manipulator, including motor dynamics with uncertain parameters in the generalized coordinate space. A dynamical adaptive sliding mode controller is designed. Liu and Li (2005) presents a sliding mode adaptive neural-network controller for trajectory following of non-holonomic mobile modular manipulators in the task space. Multilayered perceptrons (MLP) are used as estimators to approach the dynamic model of the mobile modular manipulator. Sliding mode control and a direct adaptive technique are combined to suppress bounded disturbances and modelling errors caused by parameter uncertainties. A torque compensation control is proposed for the motion control of a mobile manipulator in Chi-wu and Ke-fei (2009). By considering the modelling uncertainty and existing uncertainties disturbances, compensation is adopted for the proposed control law. Compensation is designed using the Lyapunov method. The design is validated using simulation.

In this paper, a robotic arm mounted on a non-holonomic mobile platform is considered. To solve the problems of point stabilization, trajectory tracking and path following for the mobile manipulator within a unified structure, a robust adaptive controller based on the mobile manipulator dynamics is presented. The controller design is based on a dynamic model of the mobile manipulator which accepts velocity inputs, as it is usual in commercial robots. The controller also maximizes the manipulability (Bayle & Fourquet, 2001) and provides the robot with the capability to avoid obstacles on its path. The controller design is based on two parts, each one being a controller itself. The first one is a minimum norm kinematic controller with saturation of velocity commands, which is based on the mobile manipulator's kinematics; and the second one is an adaptive dynamic compensation controller in which inputs are the velocities calculated by the kinematic controller. The adaptive dynamic compensation controller updates the estimated parameters, which are directly related to the physical parameters of the mobile manipulator. It is worth noting that in this work a single reference for the end-effector is determined, thus treating the mobile manipulator as a single coordinated system. Additionally, both stability and robustness properties to parametric uncertainties in the dynamic model are proved through Lyapunov's method. To validate the proposed control algorithms, experimental results are included and discussed.

The main contribution of this paper is the proposal of a unified controller for point stabilization, trajectory tracking and path following control of mobile manipulators. The unified controller, differently from the ones available in the references, has the advantage of solving any of the motion problems only by an adequate definition of references. The controller receives a single reference for the end-effector of the robot, and calculates the control commands as velocity references for both the platform and the arm achieving a coordinated movement of the whole system. The controller is complete, in the sense of including kinematic main and secondary motion control objectives, as well as an adaptive parameter compensation.

The paper is organized as follows: in Section 2 the kinematic and dynamic models featuring the manipulator velocities as inputs are obtained. The problem formulations both for trajectory tracking and path following are presented in Section 3. Section 4 presents the design of the kinematic controller and the adaptive dynamic compensation controller, including the stability and robustness analyses. The experimental results are presented and discussed in Section 5. Finally, conclusions are given in Section 6.

2. Mobile manipulators models

In this section, both the kinematic and the dynamic models of the mobile manipulator are presented. These two models are constructed by considering both the mobile platform and the robotic arm as parts of a unique system, according to the proposed control strategy. For this purpose, the mobile manipulator configuration is defined by a vector $\mathbf{q}=[q_1 \quad q_2 \quad \cdots \quad q_n]^T=[q_p^T \quad q_a^T]^T$ of n independent coordinates, called *generalized coordinates of the mobile manipulator*, where q_a represents the generalized coordinates of the arm, and q_p the generalized coordinates of the mobile platform. Notice that $n=n_p+n_a$, where n_a and n_p are, respectively, the dimensions of the generalized spaces associated to the robotic arm and to the mobile platform. The configuration $\mathbf{q}$ is an element of the mobile manipulator *configuration space*, denoted by $\mathcal{N}$. The location of the end-effector of the mobile manipulator is given by the m-dimensional vector of operational coordinates $\mathbf{h}=[h_1 \quad h_2 \quad \cdots \quad h_m]^T=[\mathbf{h}_{pos}^T \quad \mathbf{h}_{or}^T]^T$, where $\mathbf{h}_{pos}$ and $\mathbf{h}_{or}$ define the position and the orientation, respectively, of the end-effector in the operational space, denoted by $\mathcal{N}$. The location of the mobile manipulator end-effector can be defined in different ways according to the task, i.e., only the position of the end-effector or both its position and its orientation can be considered.

2.1. Mobile manipulator kinematic model

The *kinematic model of a mobile manipulator* gives the location of the end-effector $\mathbf{h}$ as a function of the robotic arm configuration and the platform location (or its operational coordinates as functions of the robotic arm's generalized coordinates and the mobile platform's operational coordinates) (Bayle, Fourquet, & Renaud, 2003)

$$f:\mathcal{N}_a\times\mathcal{M}_p\rightarrow\mathcal{M}$$
$$(\mathbf{q}_p,\mathbf{q}_a)\mapsto\mathbf{h}=f(\mathbf{q}_p,\mathbf{q}_a)$$

where $\mathcal{N}_a$ is the *configuration space* of the robotic arm, $\mathcal{M}_p$ is the *operational space of the platform*.

The *instantaneous kinematic model of a mobile manipulator* gives the derivative of its end-effector location as a function of the derivatives of both the robotic arm configuration and the location of the mobile platform

$$\dot{\mathbf{h}}(t)=\mathbf{J}(\mathbf{q})\mathbf{v}(t) \tag{1}$$

where $\dot{\mathbf{h}}=[\dot{h}_1 \quad \dot{h}_2 \quad \cdots \quad \dot{h}_m]^T$ is the vector of the end-effector velocity, $\mathbf{v}=[v_1 \quad v_2 \quad \cdots \quad v_{\delta_n}]^T=[v_p^T \quad v_a^T]^T$ is the vector of mobile manipulator velocities in which v_p contains the linear and angular velocities of the mobile platform and v_a contains the joint velocities of the robotic arm. The dimension of vector $\mathbf{v}$ is

$\delta_n = \delta_{np} + \delta_{na}$, where δ_{np} and δ_{na} are respectively the dimensions of the vector of velocity associated to the mobile platform and the robotic arm. Matrix

$$\mathbf{J}(\mathbf{q}) = \frac{\partial f(\mathbf{q})}{\partial \mathbf{q}} \mathbf{T}(\mathbf{q})$$

is the Jacobian matrix that defines a linear mapping between the vector of the mobile manipulator velocities $\mathbf{v}(t)$ and the vector of the end-effector velocity $\dot{\mathbf{h}}(t)$; and $\mathbf{T}(\mathbf{q})$ is the transformation matrix that relates joints velocities $\dot{\mathbf{q}}$ with mobile manipulator velocities $\mathbf{v}(t)$ such that $\dot{\mathbf{q}} = \mathbf{T}(\mathbf{q})\mathbf{v}(t)$. Note that $\mathbf{T}$ includes the non-holonomic constraints of the mobile platform. Those configurations where $\mathbf{J}(\mathbf{q})$ is rank-deficient are termed *singular kinematic configurations*. Finding the manipulator singularities is of great interest due to the following main reasons:

(1) Singularities represent configurations where the mobility of the structure is reduced, i.e., it is not possible to impose an arbitrary motion to the end-effector.
(2) In the neighbourhood of a singularity, small velocities in the operational space may cause large velocities in the $\mathbf{q}$ space.

It is to be noticed that, in general, the dimension of the operational space m is smaller than the degree of mobility δ_n of the mobile manipulator. Therefore, the system is redundant, and this characteristic should be taken into account when designing the controller to achieve some desired performance.

2.2. Mobile manipulator dynamic model

The dynamic equation of the mobile manipulator can be represented as follows (Hu & Guo, 2004):

$$\overline{\mathbf{M}}(\mathbf{q})\dot{\mathbf{v}} + \overline{\mathbf{C}}(\mathbf{q},\mathbf{v})\mathbf{v} + \overline{\mathbf{G}}(\mathbf{q}) + \overline{\mathbf{d}} = \overline{\mathbf{B}}(\mathbf{q})\boldsymbol{\tau} \tag{2}$$

where $\overline{\mathbf{M}}(\mathbf{q}) \in \Re^{\delta_n \times \delta_n}$ is a symmetrical positive definite matrix that represents the system's inertia, $\overline{\mathbf{C}}(\mathbf{q},\mathbf{v})\mathbf{v} \in \Re^{\delta_n}$ represents the components of the centripetal and Coriolis forces, $\overline{\mathbf{G}}(\mathbf{q}) \in \Re^{\delta_n}$ represent the gravitational forces, $\overline{\mathbf{d}}$ denotes bounded unknown disturbances including the unmodeled dynamics, $\boldsymbol{\tau} \in \Re^{\delta_n}$ is the torque input vector, $\overline{\mathbf{B}}(\mathbf{q}) \in \Re^{\delta_n \times \delta_n}$ is the transformation matrix of the control actions. For more details on model (2) see Hu and Guo (2004).

Most of the commercially available robots have low level PID controllers in order to follow the reference velocity inputs, thus not allowing controlling the motors directly. Therefore, it becomes useful to express more appropriately the dynamic model of the mobile manipulator by considering the rotational and longitudinal reference velocities as the input signals. With this aim, low level velocity controllers are included in the model (Andaluz, Roberti, & Carelli, 2010; De La Cruz & Carelli, 2008; De La Cruz, Freire Bastos, & Carelli, 2011)

$$\mathbf{M}(\mathbf{q})\dot{\mathbf{v}} + \mathbf{C}(\mathbf{q},\mathbf{v})\mathbf{v} + \mathbf{G}(\mathbf{q}) + \mathbf{d} = \mathbf{v}_{ref} \tag{3}$$

where, $\mathbf{M}(\mathbf{q}) = \mathbf{H}^{-1}(\overline{\mathbf{M}} + \mathbf{D})$, $\mathbf{C}(\mathbf{q},\mathbf{v}) = \mathbf{H}^{-1}(\overline{\mathbf{C}} + \mathbf{P})$, $\mathbf{G}(\mathbf{q}) = \mathbf{H}^{-1}\overline{\mathbf{G}}(\mathbf{q})$, $\mathbf{d} = \mathbf{H}^{-1}\overline{\mathbf{d}}$, $\mathbf{v}_{ref} = [\,u_{ref} \quad \omega_{ref} \quad \dot{\theta}_{1_{ref}} \quad \dot{\theta}_{2_{ref}} \quad \cdots \quad \dot{\theta}_{na_{ref}}\,]^T$.

Thus, $\mathbf{M}(\mathbf{q}) \in \Re^{\delta_n \times \delta_n}$ is a positive definite matrix representing the system's inertia, $\mathbf{C}(\mathbf{q},\mathbf{v})\mathbf{v} \in \Re^{\delta_n}$ represents the centripetal and the Coriolis forces, $\mathbf{G}(\mathbf{q}) \in \Re^{\delta_n}$ is the gravitational vector, $\mathbf{d}$ denotes bounded unknown disturbances including unmodeled dynamics and $\mathbf{v}_{ref} \in \Re^{\delta_n}$ is the vector of velocity control signals, $\mathbf{H} \in \Re^{\delta_n \times \delta_n}$, $\mathbf{D} \in \Re^{\delta_n \times \delta_n}$ and $\mathbf{P} \in \Re^{\delta_n \times \delta_n}$ are the positive definite constant diagonal matrices containing the physical parameters of the mobile manipulator, motors, and velocity controllers of both the mobile platform and the manipulator.

According to the properties of mobile manipulator model (2) (Dong, 2002; Li et al., 2008; Li, Yang, & Li, 2010), and recalling that $\mathbf{H}$, $\mathbf{D}$ and $\mathbf{P}$ are the positive definite constant diagonal matrices, the following properties for the dynamic model (3) can be straightforwardly established.

Property 1. *Matrix* $\mathbf{M}(\mathbf{q})$ *is positive definite, additionally it is known that*

$$\|\mathbf{M}(\mathbf{q})\| < k_M$$

Property 2. *The following inequality is satisfied*:

$$\|\mathbf{C}(\mathbf{q},\mathbf{v})\| < k_{c1}\|\mathbf{v}\| + k_{c2}$$

Property 3. *Vector* $\overline{\mathbf{G}}(\mathbf{q})$ *and* $\overline{\mathbf{d}}$ *are bounded*

$$\|\mathbf{G}(\mathbf{q})\| < k_G; \quad \|\mathbf{d}\| < k_d$$

where k_c, k_M,k_G *and* k_d *denote some positive constants.*

Property 4. *The dynamic model of the mobile manipulator (3) is linear in terms of a suitable selected set of parameters*

$$\mathbf{M}(\mathbf{q})\dot{\mathbf{v}} + \mathbf{C}(\mathbf{q},\mathbf{v})\mathbf{v} + \mathbf{G}(\mathbf{q}) + \mathbf{d} = \boldsymbol{\Phi}(\mathbf{q},\mathbf{v},\boldsymbol{\sigma})\boldsymbol{\chi}$$

where $\boldsymbol{\Phi}(\mathbf{q},\mathbf{v},\boldsymbol{\sigma}) \in \Re^{\delta_n \times l}$ *and* $\boldsymbol{\chi} = [\,\chi_1 \quad \chi_2 \quad \cdots \quad \chi_l\,]^T$ *is the vector of* l *unknown parameters, which are non-linear functions of the mobile manipulator's physical parameters, i.e., mass of robot, motors' constants, etc.*

For more detail about dynamic model (3) refer to Andaluz et al. (2010).

3. Problem formulation

Fundamental problems of motion control of autonomous mobile robots can be roughly classified in three groups (Soeanto, Lapierre, & Pascoal, 2003)

- *point stabilization*: the goal is to stabilize the vehicle at a given target point, with a desired orientation;
- *trajectory tracking*: the vehicle is required to track a time parameterized reference, and
- *path following*: the vehicle is required to converge to and follow a path, without any time specification.

In this work it is proposed a unified solution for the above motion control problems applied to a mobile manipulator. In this proposal it is necessary to define at any control instant both, the desired location $\mathbf{h_d}(t,s,\mathbf{h})$ and the desired velocity $\mathbf{v_{hd}}(t,s,\mathbf{h})$ of the end-effector of the mobile manipulator, which in general depend on the time t, the path variable s, and the current location of the end-effector $\mathbf{h}$. These can be represented as

$$\mathbf{h_d}(t,s,\mathbf{h}) = [\,\mathbf{h}^T_{\mathbf{d}pos} \quad \mathbf{h}^T_{\mathbf{d}or}\,]^T \tag{4}$$

$$\mathbf{v_{hd}}(t,s,\mathbf{h}) = [\,\mathbf{v}^T_{\mathbf{hd}pos} \quad \mathbf{v}^T_{\mathbf{hd}or}\,]^T \tag{5}$$

where $\mathbf{h}^T_{\mathbf{d}pos}$and $\mathbf{h}^T_{\mathbf{d}or}$ are the desired position and orientation of the end-effector, and $\mathbf{v}^T_{\mathbf{hd}pos}$ and $\mathbf{v}^T_{\mathbf{hd}or}$ represent the desired linear and angular velocities of the end-effector. In the following sections, these references $\mathbf{h_d}(t,s,\mathbf{h})$, $\mathbf{v_{hd}}(t,s,\mathbf{h})$ will be defined for each particular motion control objective.

3.1. Point stabilization

The problem of point stabilization of mobile manipulators is to drive the robot to a fixed target location. This control problem is

represented in Fig. 1. The target location is defined by the final desired position and orientation of the end-effector $\mathbf{h_d} = [\mathbf{h}_{\mathbf{d}pos}^T \quad \mathbf{h}_{\mathbf{d}or}^T]^T$. Hence, the desired location (4) and desired velocity (5) for point stabilization are defined as,

$$\mathbf{h_d}(t,s,\mathbf{h}) = \mathbf{h_d} \quad \text{(Constant)}$$
$$\mathbf{v_{hd}}(t,s,\mathbf{h}) = \dot{\mathbf{h}}_\mathbf{d} \equiv \mathbf{0}$$

The point stabilization problem is to find a feedback control law

$$\mathbf{v}_{ref}(t) = f(\tilde{\mathbf{h}}(t))$$

where $\tilde{\mathbf{h}}(t) = \mathbf{h_d} - \mathbf{h}(t)$, such that

$$\lim_{t\to\infty} \tilde{\mathbf{h}}(t) = \mathbf{0}.$$

3.2. Trajectory tracking

The trajectory tracking control problem of an autonomous robot consists of following a given time-varying trajectory $y_d(t)$ and its successive derivatives $\dot{y}_d(t)$, $\ddot{y}_d(t)$ which respectively describe the desired velocity and acceleration (Canudas de Wit, Siciliano, & Bastin, 1997). That is, the desired trajectory for the mobile manipulator is defined by a vector $\mathbf{h_d}(t,s) = [\mathbf{h}_{\mathbf{d}pos}^T \quad \mathbf{h}_{\mathbf{d}or}^T]^T$ of (5). The desired trajectory does not depend on the instantaneous position of the robot, but it is defined only by the time varying trajectory profile alone. The desired velocity $\mathbf{v_{hd}}$ is defined for this control problem as the time derivative of $\mathbf{h_d}(t,s)$, that is $\mathbf{v_{hd}} = \dot{\mathbf{h}}_\mathbf{d}(t,s) = [\dot{\mathbf{h}}_{\mathbf{d}pos}^T \quad \dot{\mathbf{h}}_{\mathbf{d}or}^T]^T$. Fig. 2 illustrates the above description of the problem. Therefore, the desired location and velocity of the end-effector (4), (5) for trajectory tracking can be defined as

$$\mathbf{h_d}(t,s,\mathbf{h}) = \mathbf{h_d}(t,s), \quad \mathbf{v_{hd}}(t,s,\mathbf{h}) = \dot{\mathbf{h}}_\mathbf{d}(t,s)$$

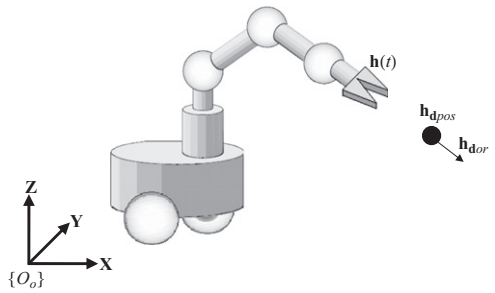

Fig. 1. Point stabilization problem. The mobile manipulator and the desired final position $\mathbf{h_d}$ are represented in the world framework $\{O_0,X,Y,Z\}$.

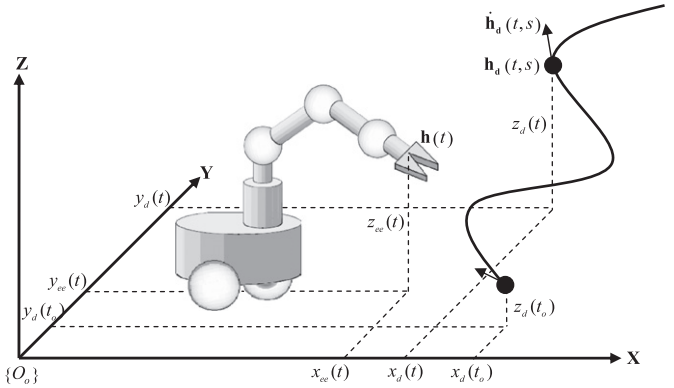

Fig. 2. Trajectory tracking problem. The mobile manipulator and the desired trajectory $\mathbf{h_d}(t,s)$ are represented in the world framework $\{O_0,X,Y,Z\}$. The initial instant t_o is used to represent the initial point of the trajectory.

Now, the trajectory control problem is to find the control actions for the mobile manipulator as a function of the control errors (position and orientation of the end-effector) and the desired velocities of the end-effector

$$\mathbf{v}_{ref}(t) = f(\tilde{\mathbf{h}}(t,s), \dot{\mathbf{h}}_\mathbf{d}(t,s))$$

such that

$$\lim_{t\to\infty} \tilde{\mathbf{h}}(t,s) = 0.$$

3.3. Path following

The solution of the path following problem for mobile robots derived in Micaelli and Samson (1993) admits an intuitive explanation. A path following controller should aim at reducing to zero both: (i) the distance from the vehicle to a point on the path, and (ii) the angle between the vehicle velocity vector and the tangent to the path at this point.

Now, it will be considered the path following problem for a mobile manipulator. As represented in Fig. 3, the path to be followed is denoted as $\mathcal{P}$. The actual desired location $\mathbf{P} = [\mathbf{p}_{pos}^T \quad \mathbf{p}_{or}^T]^T$ is defined as the closest point on $\mathcal{P}$ to the end-effector ($\mathbf{p}_{pos}$) with a desired orientation ($\mathbf{p}_{or}$), and therefore depends on both the robot position and the path. In Fig. 3, ρ represents the distance between the end-effector position $\mathbf{h}_{pos}$ and $\mathbf{p}_{pos}$, and $\tilde{\boldsymbol{\beta}} = \mathbf{p}_{or} - \mathbf{h}_{or}$ is the error orientation vector between $\mathbf{p}_{or}$ and $\mathbf{h}_{or}$. The orientation associated both to the end-effector and to the location $\mathbf{P}$ can be represented by the Euler classical angles (Paul, 1981). The desired velocity of the end-effector is defined as a velocity vector tangent to the path at the point $\mathbf{P}$, and with arbitrary module. Hence, the desired position and orientation (4), and desired velocity (5) of the end-effector of the mobile manipulator on the path $\mathcal{P}$, are defined as

$$\mathbf{h_d}(t,s,\mathbf{h}) = \mathbf{P}(t,\mathbf{h})$$
$$\mathbf{v_{hd}}(t,s,\mathbf{h}) = \boldsymbol{\upsilon}_\mathbf{P}(s,\mathbf{h})$$

where $\boldsymbol{\upsilon}_\mathbf{P}$ is the desired velocity of the end-effector at location $\mathbf{P}$. Note that the $\boldsymbol{\upsilon}_{\mathbf{P}pos}$ component of $\boldsymbol{\upsilon}_\mathbf{P}$ (20) has to be a tangent to the trajectory due to kinematics compatibility.

Given a path $\mathcal{P}$ in the operational space of the mobile manipulator and the desired velocity module υ of the end-effector, the path following control problem for mobile manipulators consists in finding a feedback control law:

$$\mathbf{v}_{ref}(t) = (s, \upsilon, \rho, \tilde{\boldsymbol{\beta}})$$

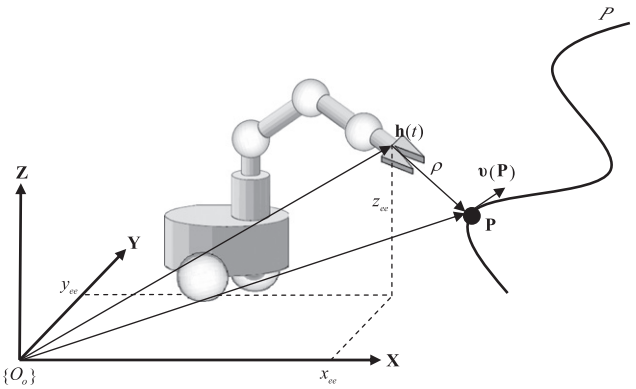

Fig. 3. Path following problem. The mobile manipulator and the desired path $\mathbf{P}(t,\mathbf{h})$ are represented in the world framework $\{O_0,X,Y,Z\}$.

such that

$$\lim_{t\to\infty}\rho(t)=0 \quad \text{and} \quad \lim_{t\to\infty}\tilde{\boldsymbol{\beta}}(t)=0$$

The error vector of position and orientation between the end-effector of the mobile manipulator and the point $\mathbf{P}$ can be represented as

$$\tilde{\mathbf{h}}=\mathbf{P}-\mathbf{h}$$

therefore, if $\lim_{t\to\infty}\tilde{\mathbf{h}}(t)=0$ then $\lim_{t\to\infty}\rho(t)=0$ and $\lim_{t\to\infty}\tilde{\beta}(t)=0$.

It is important to note that, different from the trajectory tracking and point stabilization problems, in the path following problem $\mathbf{v_{hd}}$ and $\dot{\mathbf{h}}_\mathbf{d}$ are not always equal. This is because $\mathbf{h_d}$ in not an external reference but depends on the actual robot position (the closest point on the path criterion). Therefore, if a position error exists ($\tilde{\mathbf{h}}\neq\mathbf{0}$), then the robot will perform a movement with a velocity different from $\mathbf{v_{hd}}$. Thus $\mathbf{h_d}$ will move on the path but with a velocity different from $\mathbf{v_{hd}}$ which means that $\mathbf{v_{hd}}\neq\dot{\mathbf{h}}_\mathbf{d}$. Therefore, $\mathbf{v_{hd}}$ and $\dot{\mathbf{h}}_\mathbf{d}$ will be equal only when $\tilde{\mathbf{h}}=\mathbf{0}$.

4. Controllers design

The proposed control scheme to solve the motion control problem is shown in Fig. 4. This controller can be applied to solve any of the motion control problems, that is point stabilization, trajectory tracking and path following, by an appropriate selection of the control references $\mathbf{h_d}(t,s,\mathbf{h})$ and $\mathbf{v_{hd}}(t,s,\mathbf{h})$, as has been described in Section 3. The design of the controller is based on two cascaded subsystems:

(1) Minimum norm kinematic controller with saturation of velocity commands, where its inputs are $\mathbf{h_d}(t,s,\mathbf{h})$ and $\mathbf{v_{hd}}(t,s,\mathbf{h})$ which describe the desired location and velocity of the end-effector of the mobile manipulator. The control error is defined as $\tilde{\mathbf{h}}=\mathbf{h_d}-\mathbf{h}$. Therefore, the control aim is expressed as

$$\lim_{t\to\infty}\tilde{\mathbf{h}}(t,s,\mathbf{h})=\mathbf{0}\in\Re^m$$

(2) Dynamic compensation controller, which main objective is to compensate the dynamics of the mobile manipulator thus reducing the velocity error. This controller receives as inputs the desired velocities $\mathbf{v_c}$ calculated by the kinematic controller, and generates velocity references $\mathbf{v}_{ref}$ for the mobile manipulator. The velocity control error is defined as $\tilde{\mathbf{v}}=\mathbf{v_c}\text{-}\mathbf{v}$. Hence, the control aim is to ensure that

$$\lim_{t\to\infty}\tilde{\mathbf{v}}(t)=\mathbf{0}\in\Re^{\delta_n}$$

4.1. Minimal norm kinematic controller

The design of the kinematic controller is based on the kinematic model of the mobile manipulator robot (1)

$$\dot{\mathbf{h}}=\mathbf{J}\mathbf{v}. \tag{6}$$

Now, $\mathbf{v}$ can be expressed in terms of $\dot{\mathbf{h}}$ by using the right pseudo-inverse Jacobian matrix $\mathbf{J}$

$$\mathbf{v}=\mathbf{J}^{+}\dot{\mathbf{h}}$$

where $\mathbf{J}^{+}=\mathbf{W}^{-1}\mathbf{J}^{T}(\mathbf{J}\mathbf{W}^{-1}\mathbf{J}^{T})^{-1}$, $\mathbf{W}$ being a definite positive matrix that weighs the control actions of the system

$$\mathbf{v}=\mathbf{W}^{-1}\mathbf{J}^{T}(\mathbf{J}\mathbf{W}^{-1}\mathbf{J}^{T})^{-1}\dot{\mathbf{h}} \tag{7}$$

The control law of Eq. (8) is proposed for the mobile manipulator system, which takes into account the redundancy characteristic of the robot system. The controller is based on a minimal norm solution, which means that, at any time, the mobile manipulator will attain its navigation target with the smallest number of possible movements (Sciavicco & Siciliano, 2000)

$$\mathbf{v_c}=\mathbf{J}^{+}(\mathbf{v_{hd}}+\mathbf{L_K}\tanh(\mathbf{L_K^{-1}K}\,\tilde{\mathbf{h}}))+(\mathbf{I}-\mathbf{J}^{+}\mathbf{J})\mathbf{L_D}\tanh(\mathbf{L_D^{-1}D}\,\mathbf{v}_0) \tag{8}$$

where the control action is defined as $\mathbf{v_c}=[u_c \quad \omega_c \quad \dot{\theta}_{1c} \quad \dot{\theta}_{2c} \quad \cdots \quad \dot{\theta}_{nac}]^T$. Also, in (8), $\mathbf{v_{hd}}$ is the desired velocity vector of the end-effector $\mathbf{h}$; $\tilde{\mathbf{h}}$ is the vector of control errors with $\tilde{\mathbf{h}}=\mathbf{h_d}-\mathbf{h}$; $\mathbf{I}$ is the identity matrix; $\mathbf{K}$,$\mathbf{D}$, $\mathbf{L_K}$ and $\mathbf{L_D}$ are the definite positive diagonal gain matrices; and $\mathbf{v_0}$ is an arbitrary vector which contains the velocities associated to the mobile manipulator. The first term of the right hand side in (8) describes the primary task of the end effector. The second term defines self-motion of the mobile manipulator in which matrix $(\mathbf{I}-\mathbf{J}^{+}\mathbf{J})$ projects the vector $\mathbf{v}_0$ onto the null space of the manipulator Jacobian $\mathcal{N}(\mathbf{J})$ such that the secondary control objectives do not affect the primary task of the end-effector. Therefore, any value given to $\mathbf{v}_0$will affect the internal structure of the manipulator only, but not the final control of the end-effector at all. Thus, the redundancy of the mobile manipulators can be effectively used for the achievement of additional performances such as: avoiding obstacles in the workspace, avoiding singular configurations, or to optimize various performance criteria. In this work two different secondary objectives are considered: the obstacles avoidance by the mobile platform and the singular configuration prevention through the system's manipulability control. These secondary objectives are described below.

In order to include an analytical saturation of control velocities, the $\tanh(\cdot)$ functions are included. Thus Eq. (8) remains bounded, and gains in $\mathbf{L_K}$ and $\mathbf{L_D}$ are selected such that the control action $\mathbf{v_c}$ be guaranteed to remain lower than the maximum admissible velocity values in the robot. On the other hand, $\mathbf{K}$ and $\mathbf{D}$ are selected as adequate gains for a good performance with small control errors. The expressions $\tanh(\mathbf{L_K^{-1}K}\,\tilde{\mathbf{h}})$ and $\tanh(\mathbf{L_D^{-1}Dv_0})$ denote a component by component operation.

4.2. Manipulability

It can be observed that one of the main requirements for an accurate task execution by the robot is a good manipulability, defined as the robot configuration that maximizes its ability to manipulate a target object. Therefore, one of the secondary

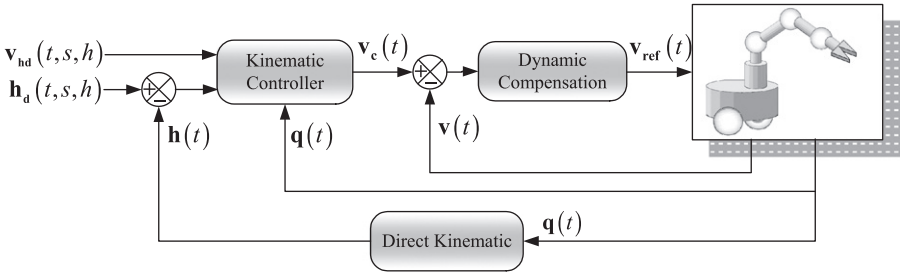

Fig. 4. Block diagram of the motion control system for mobile manipulators.

objectives of the control is to maintain maximum manipulability of the mobile manipulator during task execution. Manipulability is a concept useful to measure the ability of a fixed manipulator to move in certain directions (Yoshikawa, 1985). Bayle and Fourquet (2001) present a similar analysis for the manipulability of mobile manipulators and extend the concept of manipulability ellipsoid as the set of all end-effector velocities reachable by robot velocities $\mathbf{v}$ satisfying $\|\mathbf{v}\| \leq 1$ in the Euclidean space. A global representative measure of manipulation ability can be obtained by considering the volume of this ellipsoid which is proportional to the quantity w called the *manipulability measure*,

$$w = \sqrt{\det\left(\mathbf{J}(\mathbf{q})\mathbf{J}^T(\mathbf{q})\right)} \tag{9}$$

Therefore, the mobile manipulator will have maximum manipulability if its internal configuration is such that it maximizes the manipulability measure w. This way, if the mobile manipulator maintains a high manipulability while performing its movements, then the possibility of attaining a singular configuration is reduced.

4.3. Obstacle avoidance

The main idea is to avoid obstacles where maximum height does not interfere with the robotic arm. Therefore the arm can follow the desired path while the mobile platform avoids the obstacle by resourcing to the null space configuration. Fig. 5 shows the obstacle avoidance strategy. The angular velocity and the longitudinal velocity of the mobile platform will be affected by a fictitious repulsion force. This force depends on the incidence angle on the obstacle α, and the distance d to the obstacle. This way, the following control velocities of the mobile platform are proposed when the robot enters the interaction zone

$$u_{obs} = Z^{-1}(k_{uobs}(r-d)[\pi/2-|\alpha|]) \tag{10}$$

$$\omega_{obs} = Z^{-1}(k_{\omega obs}(r-d)\mathrm{sign}(\alpha)[\pi/2-|\alpha|]) \tag{11}$$

where r is the radius of the interaction zone which determines the distance at which the obstacle starts to be avoided, $k_{u\,obs}$ and $k_{\omega\,obs}$ are positive adjustment gains, the sign function allows defining to which side the obstacle is to be avoided being $\mathrm{sign}(0)=1$. Z represents the mechanical impedance characterizing the robot–environment interaction, which is calculated as $Z = Ip^2+Bp+K$; with p the derivative operator and I, B and K being positive constants representing, respectively, the effect of the inertia, the damping and the elasticity. The closer the platform is to the obstacle, the bigger the values of ω_{obs} and u_{obs}.

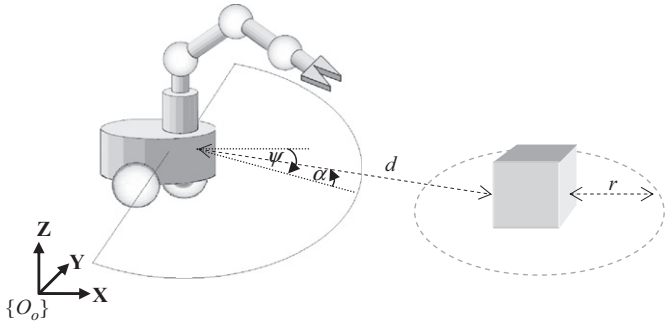

Fig. 5. Obstacle evasion scheme. The mobile manipulator and the obstacle are represented in the world framework $\{O_0,X,Y,Z\}$. The interaction zone of radius r, distance d, and incidence angle α are also represented.

Taking into account the maximum manipulability (9) and the obstacle avoidance (10) and (11), the vector $\mathbf{v}_0$ is now defined as

$$\mathbf{v}_0 = [\,-u_{obs} \quad \omega_{obs} \quad k_{v1}(\theta_{1d}-\theta_1) \quad k_{v2}(\theta_{2d}-\theta_2) \quad \cdots \quad k_{vna}(\theta_{nad}-\theta_{na})\,]^T \tag{12}$$

where $k_{vi}(\theta_{id}-\theta_i)$ with $i=1,2,\ldots,n_a$ and $k_{vi}>0$ are the joint velocities proportional to the configuration errors of the mobile robotic arm, in such a way that the manipulator joints will be pulled to the desired θ_{id} values that maximize manipulability. Note that $-u_{obs}$ represents a reduction value of the linear velocity in order to obtain a cautious behaviour. For this reason, u_{obs} must be subtracted from the linear velocity component obtained in the first term of (8).

4.4. Stability analysis of the kinematic controller

Theorem 1. *Let us consider the kinematic model for the mobile manipulator (6) and the proposed control law (8), and assume perfect velocity tracking*, i.e. $\mathbf{v} \equiv \mathbf{v_c}$. *Then,* $\tilde{\mathbf{h}}(t) \to \mathbf{0}$ *with* $t \to \infty$ *for all motion problems.*

Proof. By considering the hypothesis of perfect velocity tracking, that is $\mathbf{v} \equiv \mathbf{v_c}$, (8) can be substituted in (6) to obtain the following close loop equation:

$$(\mathbf{v_{hd}} - \dot{\mathbf{h}}) + \mathbf{L_K}\tanh(\mathbf{L_K^{-1}K}\,\tilde{\mathbf{h}}) = \mathbf{0} \tag{13}$$

Remember that, in general, the desired velocity vector $\mathbf{v_{hd}}$ is different from the time derivative of the desired location $\dot{\mathbf{h}}_\mathbf{d}$. Now, defining the difference signal Υ

$$\Upsilon = \dot{\mathbf{h}}_\mathbf{d} - \mathbf{v_{hd}} \tag{14}$$

and remembering that $\dot{\tilde{\mathbf{h}}} = \dot{\mathbf{h}}_\mathbf{d} - \dot{\mathbf{h}}$, (13) can be written as

$$\dot{\tilde{\mathbf{h}}} + \mathbf{L_K}\tanh(\mathbf{L_K^{-1}K}\,\tilde{\mathbf{h}}) = \Upsilon \tag{15}$$

Note that $\mathbf{v_{hd}}$ is collinear to $\dot{\mathbf{h}}_\mathbf{d}$ (tangent to the path), then Υ is also a collinear vector to $\mathbf{v_{hd}}$ and $\dot{\mathbf{h}}_\mathbf{d}$.

Now, for the stability proof, the following Lyapunov candidate function is considered:

$$V(\tilde{\mathbf{h}}) = \tfrac{1}{2}\tilde{\mathbf{h}}^\mathbf{T}\tilde{\mathbf{h}} \tag{16}$$

Its time derivative on the trajectories of the system is

$$\dot{V}(\tilde{\mathbf{h}}) = \tilde{\mathbf{h}}^\mathbf{T}\Upsilon - \tilde{\mathbf{h}}^\mathbf{T}\mathbf{L_K}\tanh(\mathbf{L_K^{-1}K}\,\tilde{\mathbf{h}}) \tag{17}$$

A sufficient condition for $\dot{V}(\tilde{\mathbf{h}})$ to be negative definite is

$$|\tilde{\mathbf{h}}^\mathbf{T}\mathbf{L_K}\tanh(\mathbf{L_K^{-1}K}\,\tilde{\mathbf{h}})| > |\tilde{\mathbf{h}}^\mathbf{T}\Upsilon| \tag{18}$$

For large values of $\tilde{\mathbf{h}}$, the condition in (18) can be reinforced as

$$\|\tilde{\mathbf{h}}^T\,\mathbf{L'_K}\| > \|\tilde{\mathbf{h}}\|\,\|\Upsilon\| \tag{19}$$

with $\mathbf{L'_K} = \mathbf{L_K}\tanh(k_{aux}\mathbf{i})$, where k_{aux} is a suitable positive constant and $\mathbf{i} \in R^m$ is the vector of unity components (see Fig. 6). Then, $\dot{V}$ will be negative definite only if

$$\|\mathbf{L_K}\| > \frac{\|\Upsilon\|}{\tanh(k_{aux})} \tag{20}$$

Hence, (20) establishes a design condition to make the errors $\tilde{\mathbf{h}}$ to decrease.

Now, for small values of $\tilde{\mathbf{h}}$, condition (18) will be fulfilled if (see Fig. 6)

$$\|\tilde{\mathbf{h}}^T\,\mathbf{K}\frac{\tanh(k_{aux})}{k_{aux}}\tilde{\mathbf{h}}\| > \|\tilde{\mathbf{h}}\|\,\|\Upsilon\| \tag{21}$$

which means that a sufficient condition for $\dot{V}$ to be negative definite is

$$\|\tilde{\mathbf{h}}\| > k_{aux}\frac{\|\Upsilon\|}{\lambda_{min}(\mathbf{K})\tanh(k_{aux})} \tag{22}$$

Thus implying that the error $\tilde{\mathbf{h}}$ is ultimately bounded by

$$\|\tilde{\mathbf{h}}\| \leq \frac{k_{aux}\|\Upsilon\|}{\varsigma\lambda_{min}(\mathbf{K})\tanh(k_{aux})} \quad \text{with } 0<\varsigma<1 \tag{23}$$

Let us now analyse the bound in (23) for the different control objectives.

Case 1. For the case of point stabilization, the desired velocity is $\mathbf{v_{hd}}=\dot{\mathbf{h}}_\mathbf{d}\equiv\mathbf{0}$ then $\Upsilon\equiv\mathbf{0}$, which implies by condition (23) that the location error of the end-effector verifies $\tilde{\mathbf{h}}(t)\to\mathbf{0}$ asymptotically.

Case 2. For the case of trajectory tracking, the desired velocity is $\mathbf{v_{hd}}\equiv\dot{\mathbf{h}}_\mathbf{d}$ then $\Upsilon\equiv\mathbf{0}$, thus the location error of the end-effector verifies $\tilde{\mathbf{h}}(t)\to\mathbf{0}$ asymptotically.

Case 3. For the case of path following, the desired velocity is $\mathbf{v_{hd}}=\dot{\mathbf{h}}_\mathbf{d}-\Upsilon$. Once the control error is inside the bound (23), that is with small values of $\tilde{\mathbf{h}}$, $\mathbf{L_K}\tanh(\mathbf{L_K^{-1}K}\ \tilde{\mathbf{h}}\ )\approx\mathbf{K}\tilde{\mathbf{h}}$. Now, it is proved by contradiction that this control error tends to zero. The closed loop Eq. (15) can be written as

$$\dot{\tilde{\mathbf{h}}}+\mathbf{K}\,\tilde{\mathbf{h}}=\Upsilon \tag{24}$$

or after the transient, in Laplace transform

$$\tilde{\mathbf{h}}(s)=(s\mathbf{I}+\mathbf{K})^{-1}\,\Upsilon(s) \tag{25}$$

According to (25) and recalling that $\mathbf{K}$ is a diagonal positive definite, the control error vector $\tilde{\mathbf{h}}$ and the velocity vector Υ cannot be orthogonal. Nevertheless both vectors are orthogonal by definition (see Note 1 and remember the minimum distance criteria for $\mathbf{h_d}$ on $\mathbf{P}$). Therefore the only solution for steady state is that $\tilde{\mathbf{h}}(t)\to\mathbf{0}$ asymptotically. □

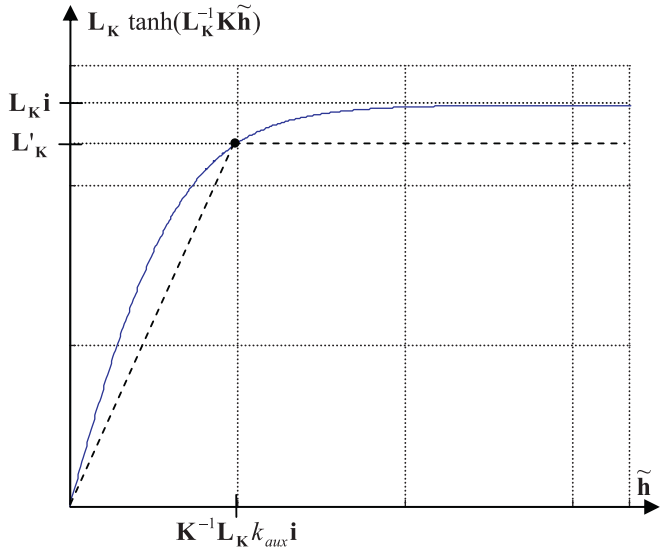

Fig. 6. Saturation function tanh(·) as solid line, and linear functions below tanh(·) as dash line.

4.5. Dynamic compensation

The objective of the dynamic compensation controller is to compensate for the dynamics of the mobile manipulator robot, thus reducing the velocity tracking error. This controller receives as inputs the desired velocities $\mathbf{v_c}$ calculated by the kinematic controller, and generates velocity references $\mathbf{v}_{ref}$ for the mobile manipulator robot (see Fig. 4). Hence, if there is no perfect velocity tracking, the velocity error is defined as

$$\tilde{\mathbf{v}}=\mathbf{v_c}-\mathbf{v} \tag{26}$$

This velocity error motivates the dynamic compensation process, which will be performed based on the inverse dynamics of the mobile manipulator. The uncertainties in the dynamic parameters of the robot motivate to design an ***adaptive dynamic compensation controller*** with a robust parameter updating law, Fig. 7.

With this aim, the following control law is proposed:

$$\mathbf{v}_{ref}=\hat{\mathbf{M}}(\mathbf{q})\boldsymbol{\sigma}+\hat{\mathbf{C}}(\mathbf{q},\mathbf{v})\mathbf{v_c}+\hat{\mathbf{G}}(\mathbf{q}) \tag{27}$$

where $\mathbf{v}_{ref}=[\,u_{ref}\quad \omega_{ref}\quad \dot{\theta}_{1ref}\quad \dot{\theta}_{2ref}\quad \cdots\quad \dot{\theta}_{na\ ref}\,]^T$ is the control action and

$$\boldsymbol{\sigma}=\dot{\mathbf{v}}_\mathbf{c}+\mathbf{L_v}\tanh(\mathbf{L_v^{-1}K_v}\tilde{\mathbf{v}}) \tag{28}$$

with $\mathbf{K_v}$ and $\mathbf{L_v}$ as the diagonal positive definite matrices.

For the sake of simplicity, from now on the following will be written $\mathbf{M}=\mathbf{M}(\mathbf{q})$, $\mathbf{C}=\mathbf{C}(\mathbf{q},\mathbf{v})$ and

$$\mathbf{G}=\mathbf{G}(\mathbf{q})$$

Considering *Property 4*, the control law (27) can be written as

$$\mathbf{v}_{ref}=\boldsymbol{\Phi}\hat{\boldsymbol{\chi}}=\boldsymbol{\Phi}\boldsymbol{\chi}+\boldsymbol{\Phi}\tilde{\boldsymbol{\chi}}=\mathbf{M}\boldsymbol{\sigma}+\mathbf{C}\mathbf{v_c}+\mathbf{G}+\boldsymbol{\Phi}\tilde{\boldsymbol{\chi}} \tag{29}$$

where $\boldsymbol{\Phi}(\mathbf{q},\mathbf{v},\boldsymbol{\sigma})\in\Re^{\delta_n\ \mathrm{x}\ l}$ and $\boldsymbol{\chi}$, $\hat{\boldsymbol{\chi}}$ are the real and estimated parameters of the mobile manipulator, respectively, whereas $\tilde{\boldsymbol{\chi}}=\hat{\boldsymbol{\chi}}-\boldsymbol{\chi}$ is the vector of parameter errors.

Also, the following parameter-updating law is proposed. It is based on a leakage term, or σ-modification (Kaufman et al., 1998;

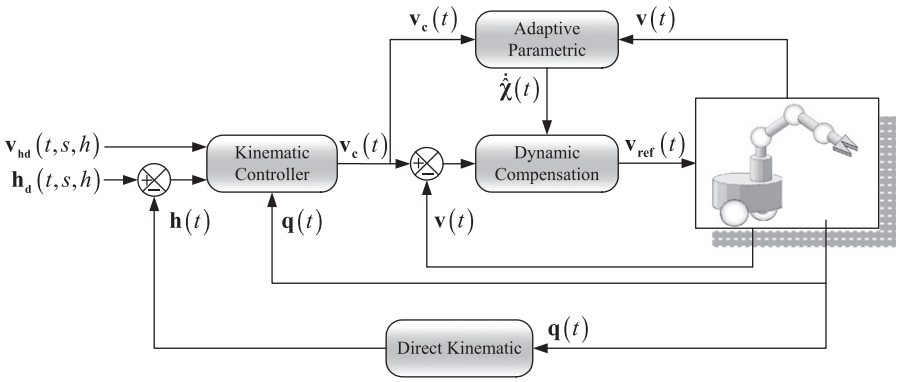

Fig. 7. Block diagram of the proposed adaptive dynamic control system.

Sastry and Bodson, 1989). Nasisi and Carelli (2003) presented an adaptive visual servo controller with σ-modification applied to a robot manipulator. By including such term, the robust updating law is obtained

$$\dot{\hat{\boldsymbol{\chi}}} = \boldsymbol{\gamma}^{-1}\boldsymbol{\Phi}^{\mathbf{T}}\mathbf{H}\tilde{\mathbf{v}} - \boldsymbol{\gamma}^{-1}\boldsymbol{\Gamma}\hat{\boldsymbol{\chi}} \tag{30}$$

where $\boldsymbol{\Gamma} \in \Re^{l\,x\,l}$ is a diagonal positive gain matrix. Eq. (30) is rewritten as

$$\dot{\tilde{\boldsymbol{\chi}}} = \boldsymbol{\gamma}^{-1}\boldsymbol{\Phi}^{\mathbf{T}}\mathbf{H}\tilde{\mathbf{v}} - \boldsymbol{\gamma}^{-1}\boldsymbol{\Gamma}\tilde{\boldsymbol{\chi}} - \boldsymbol{\gamma}^{-1}\boldsymbol{\Gamma}\boldsymbol{\chi} \tag{31}$$

Theorem 2. *Let us consider the control law (29) and the update law (31) in closed loop with the robot's dynamic model (3). Then, the velocity error $\tilde{\mathbf{v}}(t)$ and the parameter errors $\tilde{\boldsymbol{\chi}}(t)$ are ultimately bounded.*

Proof. Equating (3) and (29), the closed-loop equation is obtained:

$$\mathbf{M}\dot{\mathbf{v}} + \mathbf{C}\mathbf{v} + \mathbf{G} = \mathbf{M}\boldsymbol{\sigma} + \mathbf{C}\mathbf{v}_{\mathbf{c}} + \mathbf{G} + \boldsymbol{\Phi}\tilde{\boldsymbol{\chi}} \quad \mathbf{M}(\boldsymbol{\sigma} - \dot{\mathbf{v}}) = -\mathbf{C}\tilde{\mathbf{v}} - \boldsymbol{\Phi}\tilde{\boldsymbol{\chi}} \tag{32}$$

Substituting (28) in (32)

$$\dot{\tilde{\mathbf{v}}} = -\mathbf{M}^{-1}\boldsymbol{\Phi}\tilde{\boldsymbol{\chi}} - \mathbf{M}^{-1}\mathbf{C}\tilde{\mathbf{v}} - \mathbf{L}_{\mathbf{v}}\tanh(\mathbf{L}_{\mathbf{v}}^{-1}\mathbf{K}_{\mathbf{v}}\tilde{\mathbf{v}}) \tag{33}$$

A Lyapunov candidate function is proposed as

$$V(\tilde{\mathbf{v}}, \tilde{\boldsymbol{\chi}}) = \tfrac{1}{2}\tilde{\mathbf{v}}^{\mathbf{T}}\mathbf{H}\mathbf{M}\tilde{\mathbf{v}} + \tfrac{1}{2}\tilde{\boldsymbol{\chi}}^{\mathbf{T}}\boldsymbol{\gamma}\tilde{\boldsymbol{\chi}} \tag{34}$$

where $\boldsymbol{\gamma} \in \Re^{l\,x\,l}$ is a positive definite diagonal matrix and $\mathbf{HM}$ is a symmetric and positive definite matrix. The time derivative of the Lyapunov candidate function on the system's trajectories is

$$\dot{V}(\tilde{\mathbf{v}}, \tilde{\boldsymbol{\chi}}) = -\tilde{\mathbf{v}}^{\mathbf{T}}\mathbf{H}\mathbf{M}\mathbf{L}_{\mathbf{v}}\tanh(\mathbf{L}_{\mathbf{v}}^{-1}\mathbf{K}_{\mathbf{v}}\tilde{\mathbf{v}}) - \tilde{\mathbf{v}}^{\mathbf{T}}\mathbf{H}\mathbf{C}\tilde{\mathbf{v}} - \tilde{\mathbf{v}}^{\mathbf{T}}\mathbf{H}\boldsymbol{\Phi}\tilde{\boldsymbol{\chi}} + \tilde{\boldsymbol{\chi}}^{\mathbf{T}}\boldsymbol{\gamma}\tilde{\boldsymbol{\chi}} + \tfrac{1}{2}\tilde{\mathbf{v}}^{\mathbf{T}}\mathbf{H}\dot{\mathbf{M}}\tilde{\mathbf{v}}$$

Now, recalling that $\mathbf{M}(\mathbf{q}) = \mathbf{H}^{-1}(\overline{\mathbf{M}} + \mathbf{D})$ and $\mathbf{C}(\mathbf{q}, \mathbf{v}) = \mathbf{H}^{-1}(\overline{\mathbf{C}} + \mathbf{P})$,

$$\dot{V}(\tilde{\mathbf{v}}, \tilde{\boldsymbol{\chi}}) = -\tilde{\mathbf{v}}^{\mathbf{T}}\mathbf{H}\mathbf{M}\mathbf{L}_{\mathbf{v}}\tanh(\mathbf{L}_{\mathbf{v}}^{-1}\mathbf{K}_{\mathbf{v}}\tilde{\mathbf{v}}) - \tilde{\mathbf{v}}^{\mathbf{T}}(\overline{\mathbf{C}} + \mathbf{P})\tilde{\mathbf{v}} - \tilde{\mathbf{v}}^{\mathbf{T}}\mathbf{H}\boldsymbol{\Phi}\tilde{\boldsymbol{\chi}} + \tilde{\boldsymbol{\chi}}^{\mathbf{T}}\boldsymbol{\gamma}\tilde{\boldsymbol{\chi}} + \tfrac{1}{2}\tilde{\mathbf{v}}^{\mathbf{T}}\dot{\overline{\mathbf{M}}}\tilde{\mathbf{v}}$$

Due to the well known skew-symmetric property of $(\dot{\overline{\mathbf{M}}} - 2\overline{\mathbf{C}})$, $\dot{V}(\tilde{\mathbf{v}}, \tilde{\boldsymbol{\chi}})$ reduces to

$$\dot{V}(\tilde{\mathbf{v}}, \tilde{\boldsymbol{\chi}}) = -\tilde{\mathbf{v}}^{\mathbf{T}}\mathbf{H}\mathbf{M}\mathbf{L}_{\mathbf{v}}\tanh(\mathbf{L}_{\mathbf{v}}^{-1}\mathbf{K}_{\mathbf{v}}\tilde{\mathbf{v}}) - \tilde{\mathbf{v}}^{\mathbf{T}}\mathbf{P}\tilde{\mathbf{v}} - \tilde{\mathbf{v}}^{\mathbf{T}}\mathbf{H}\boldsymbol{\Phi}\tilde{\boldsymbol{\chi}} + \tilde{\boldsymbol{\chi}}^{\mathbf{T}}\boldsymbol{\gamma}\tilde{\boldsymbol{\chi}} \tag{35}$$

Let us consider that the dynamic parameters can vary, i.e., $\chi = \chi(t)$ and $\dot{\tilde{\boldsymbol{\chi}}} = \dot{\hat{\boldsymbol{\chi}}} - \dot{\boldsymbol{\chi}}$. Substituting (31) in (35)

$$\dot{V}(\tilde{\mathbf{v}}, \tilde{\boldsymbol{\chi}}) = -\tilde{\mathbf{v}}^{\mathbf{T}}\mathbf{H}\mathbf{M}\mathbf{L}_{\mathbf{v}}\tanh(\mathbf{L}_{\mathbf{v}}^{-1}\mathbf{K}_{\mathbf{v}}\tilde{\mathbf{v}}) - \tilde{\mathbf{v}}^{\mathbf{T}}\mathbf{P}\tilde{\mathbf{v}} - \tilde{\boldsymbol{\chi}}^{\mathbf{T}}\boldsymbol{\Gamma}\tilde{\boldsymbol{\chi}} - \tilde{\boldsymbol{\chi}}^{\mathbf{T}}\boldsymbol{\Gamma}\boldsymbol{\chi} - \tilde{\boldsymbol{\chi}}^{\mathbf{T}}\boldsymbol{\gamma}\boldsymbol{\chi}. \tag{36}$$

Considering small values of $\tilde{\mathbf{v}}$, then $\mathbf{L}_{\mathbf{v}}\tanh(\mathbf{L}_{\mathbf{v}}^{-1}\mathbf{K}_{\mathbf{v}}\tilde{\mathbf{v}}) \approx \mathbf{K}_{\mathbf{v}}\tilde{\mathbf{v}}$. The following constants are defined: $\upsilon_{\Gamma} = k_{max}(\boldsymbol{\Gamma})$, $\upsilon_{\gamma} = k_{max}(\boldsymbol{\gamma})$, $\mu_{\Gamma} = \chi(\boldsymbol{\Gamma})$, $\mu_{MK_vP} = \chi(\mathbf{HMK_v}) + \chi(\mathbf{P})$, where $\chi(\mathbf{Z}) = \sqrt{\lambda_{min}(\mathbf{Z}^{\mathbf{T}}\mathbf{Z})}$ is the minimum singular value to $\mathbf{Z}$, $k_{max}(\mathbf{Z}) = \sqrt{\lambda_{max}(\mathbf{Z}^{\mathbf{T}}\mathbf{Z})}$ denotes the maximum singular value of $\mathbf{Z}$, and $\lambda_{min}(\cdot)$ and $\lambda_{max}(\cdot)$ represent the smallest and the biggest eigenvalues of a matrix, respectively. Then, $\dot{V}$ can be rewritten as

$$\dot{V}(\tilde{\mathbf{v}}, \tilde{\boldsymbol{\chi}}) = -\mu_{MK_vP}\|\tilde{\mathbf{v}}\|^2 - \mu_{\Gamma}\|\tilde{\boldsymbol{\chi}}\|^2 + \upsilon_{\Gamma}\|\tilde{\boldsymbol{\chi}}\|\|\boldsymbol{\chi}\| + \upsilon_{\gamma}\|\tilde{\boldsymbol{\chi}}\|\|\dot{\boldsymbol{\chi}}\|. \tag{37}$$

Considering $\zeta \in \Re^+$ is a difference square

$$\left(\frac{1}{\zeta}\|\tilde{\boldsymbol{\chi}}\| - \zeta\|\boldsymbol{\chi}\|\right)^2 = \frac{1}{\zeta^2}\|\tilde{\boldsymbol{\chi}}\|^2 - 2\|\tilde{\boldsymbol{\chi}}\|\|\boldsymbol{\chi}\| + \zeta^2\|\boldsymbol{\chi}\|^2$$

can be written as

$$\|\tilde{\boldsymbol{\chi}}\|\|\boldsymbol{\chi}\| \leq \frac{1}{2\zeta^2}\|\tilde{\boldsymbol{\chi}}\|^2 + \frac{\zeta^2}{2}\|\boldsymbol{\chi}\|^2. \tag{38}$$

By applying a similar reasoning with $\eta \in \Re^+$, the following can be obtained:

$$\|\tilde{\boldsymbol{\chi}}\|\|\dot{\boldsymbol{\chi}}\| \leq \frac{1}{2\eta^2}\|\tilde{\boldsymbol{\chi}}\|^2 + \frac{\eta^2}{2}\|\dot{\boldsymbol{\chi}}\|^2. \tag{39}$$

Substituting (38) and (39) in (37)

$$\dot{V}(\tilde{\mathbf{v}}, \tilde{\boldsymbol{\chi}}) \leq -\mu_{MK_vP}\|\tilde{\mathbf{v}}\|^2 - \mu_{\Gamma}\|\tilde{\boldsymbol{\chi}}\|^2 + \upsilon_{\Gamma}\left(\frac{1}{2\zeta^2}\|\tilde{\boldsymbol{\chi}}\|^2 + \frac{\zeta^2}{2}\|\boldsymbol{\chi}\|^2\right) + \upsilon_{\gamma}\left(\frac{1}{2\eta^2}\|\tilde{\boldsymbol{\chi}}\|^2 + \frac{\eta^2}{2}\|\dot{\boldsymbol{\chi}}\|^2\right). \tag{40}$$

Eq. (40) can be written in compact form as

$$\dot{V}(\tilde{\mathbf{v}}, \tilde{\boldsymbol{\chi}}) \leq -\varepsilon_1\|\tilde{\mathbf{v}}\|^2 - \varepsilon_2\|\tilde{\boldsymbol{\chi}}\|^2 + \delta \tag{41}$$

where $\varepsilon_1 = \mu_{MK_vP} > 0$, $\varepsilon_2 = \mu_{\Gamma} - (\upsilon_{\Gamma}/2\zeta^2) - (\upsilon_{\gamma}/2\eta^2) > 0$ and $\delta = \upsilon_{\Gamma}(\zeta^2/2)\|\boldsymbol{\chi}\|^2 + \upsilon_{\gamma}(\eta^2/2)\|\dot{\boldsymbol{\chi}}\|^2$, with ζ and η conveniently selected. Now, from the Lyapunov candidate function $V(\tilde{\mathbf{v}}, \tilde{\boldsymbol{\chi}}) = \frac{1}{2}\tilde{\mathbf{v}}^{\mathbf{T}}\mathbf{H}\mathbf{M}\tilde{\mathbf{v}} + \frac{1}{2}\tilde{\boldsymbol{\chi}}^{\mathbf{T}}\boldsymbol{\gamma}\tilde{\boldsymbol{\chi}}$ it can be stated that

$$V \leq \beta_1\|\tilde{\mathbf{v}}\|^2 + \beta_2\|\tilde{\boldsymbol{\chi}}\|^2 \tag{42}$$

where $\beta_1 = \frac{1}{2}\vartheta_{\overline{M}}$, $\beta_2 = \frac{1}{2}\vartheta_{\gamma}$, $\vartheta_{\overline{M}} = k_{max}(\mathbf{HM})$, $\vartheta_{\gamma} = k_{max}(\boldsymbol{\gamma})$. Then

$$\dot{V} \leq -\Lambda V + \delta \tag{43}$$

with $\Lambda = \varepsilon_1/\beta_1, \varepsilon_2/\beta_2$. Since δ is bounded, (43) implies that $\tilde{\mathbf{v}}(t)$ and $\tilde{\boldsymbol{\chi}}(t)$ are finally bounded. □

Note 1: The term δ is a function of the minimum singular value of the gain matrix $\boldsymbol{\Gamma}$ of the σ-modification term, thus it can be made small by appropriately selecting this matrix. Also note that the proposed adaptive dynamic controller does not guarantee that $\tilde{\boldsymbol{\chi}} \to 0$ as $t \to \infty$. In other words, estimated parameters might converge to values that are different from their true values. Actually, it is not required that $\tilde{\boldsymbol{\chi}} \to 0$ in order to make $\tilde{\mathbf{v}}(t)$ converge to a bounded value.

Note 2: Note that the updating law (31) needs the $\mathbf{H}$ matrix. This matrix includes parameters of the actuators, which can be easily known and remain constant. Therefore, this is not a relevant constraint within the adaptive control design.

The behaviour of the control error of the end-effector $\mathbf{h}$ is now analysed relaxing the assumption of perfect velocity tracking which was considered in *Theorem 1* for the kinematic controller.

Theorem 3. *Let us consider the proposed control law (8) in close loop with the kinematic model of the mobile manipulator (6). Then, the control error vector of the end-effector $\tilde{\mathbf{h}}(t)$ is ultimately bounded for all motion problems.*

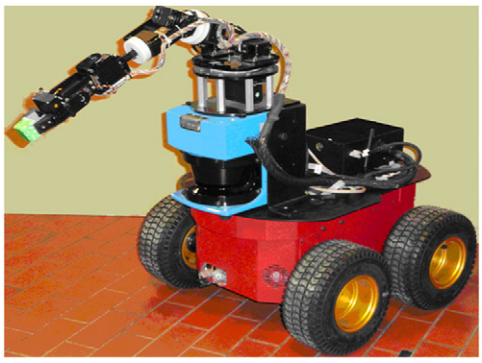

Fig. 8. Mobile manipulator used in the experiments. Mobile platform Pioneer 3-AT, and robotic arm Cyton Alpha 7 dof.

Proof. Disregarding the assumption of perfect velocity tracking, closed loop Eq. (15) can now be written as

$$\dot{\tilde{\mathbf{h}}} + \mathbf{L_K} \tanh(\mathbf{L_K^{-1}} \mathbf{K} \tilde{\mathbf{h}}) = \mathbf{J}\tilde{\mathbf{v}} + \Upsilon \tag{44}$$

A Lyapunov candidate function (16) is considered, whose time derivative on the system's trajectories is

$$\dot{V}(\tilde{\mathbf{h}}) = \tilde{\mathbf{h}}^{\mathbf{T}}(\mathbf{J}\tilde{\mathbf{v}} + \Upsilon) - \tilde{\mathbf{h}}^{\mathbf{T}} \mathbf{L_K} \tanh(\mathbf{L_K^{-1}} \mathbf{K} \tilde{\mathbf{h}}) \tag{45}$$

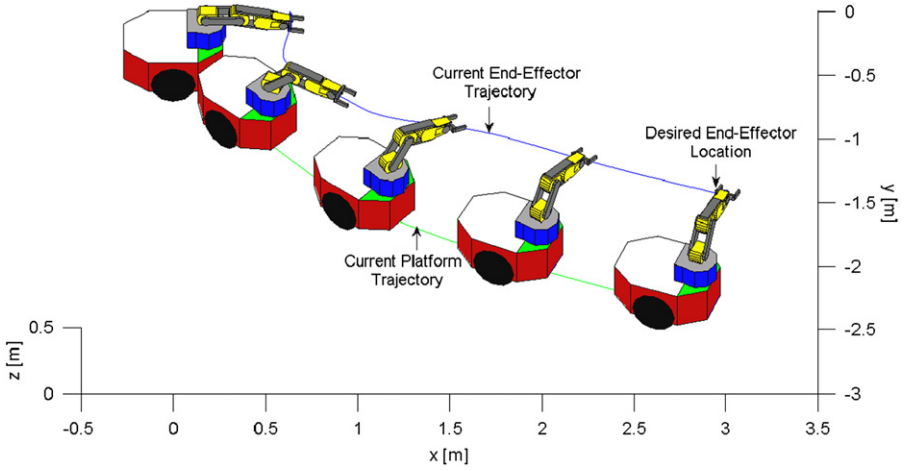

Fig. 9. Stroboscopic movement of the mobile manipulator in the point stabilization experiment.

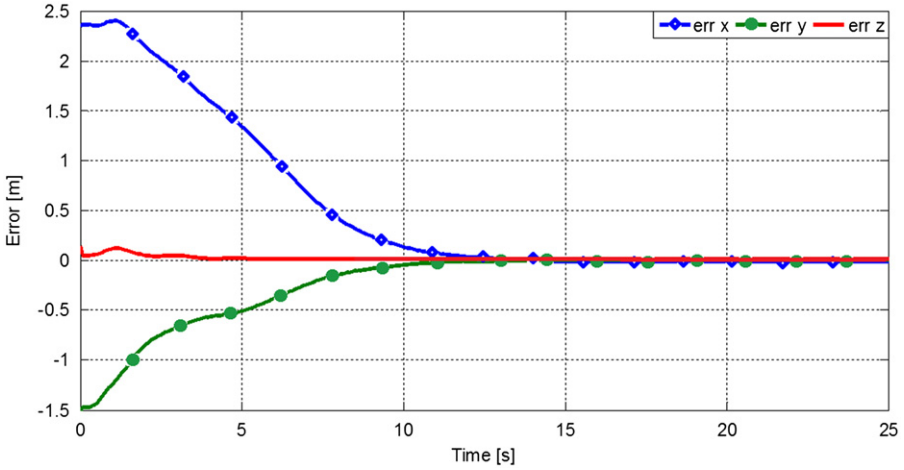

Fig. 10. Kinematic control errors $\tilde{\mathbf{h}}$ in the point stabilization experiment.

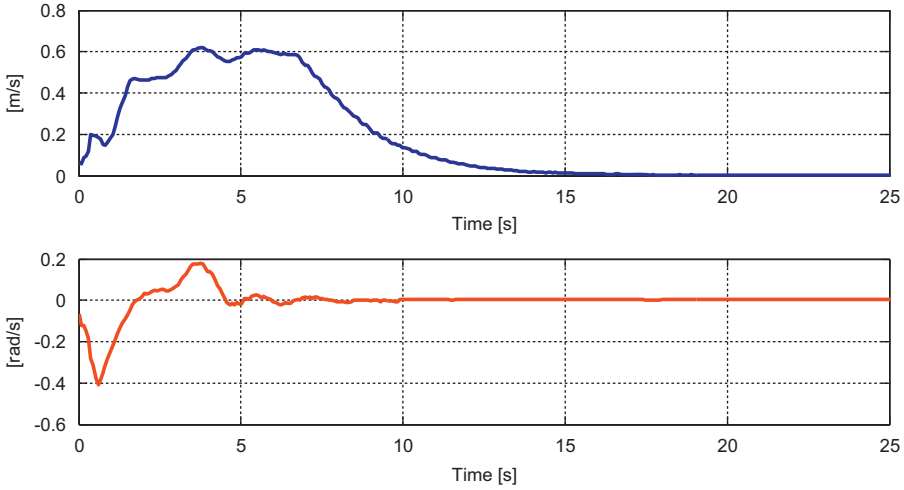

Fig. 11. Velocity commands to the mobile platform in the point stabilization experiment. Linear velocity command in the upper graph and angular velocity command in the lower graph.

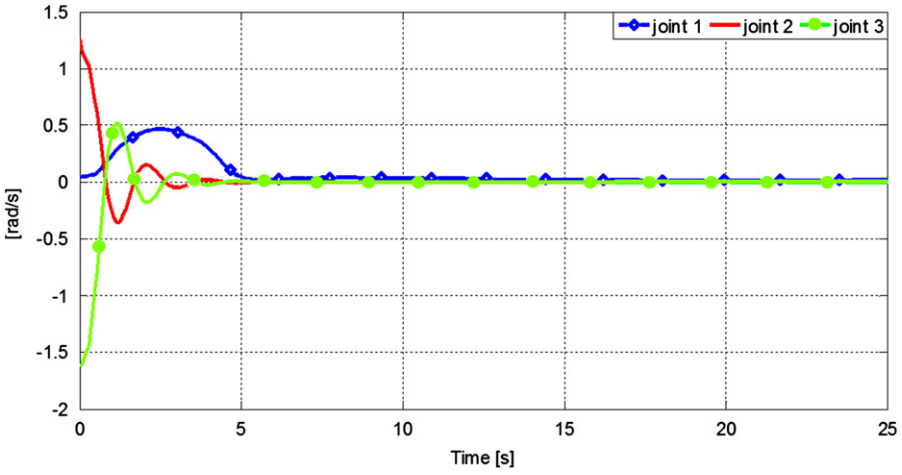

Fig. 12. Joint velocity commands for the robotic arm in the point stabilization experiment.

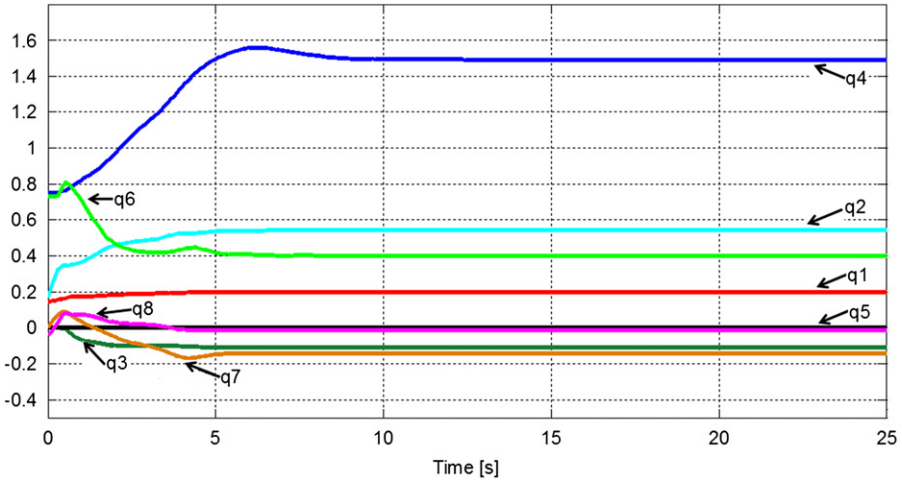

Fig. 13. Adaptive parameters evolution in the point stabilization experiment.

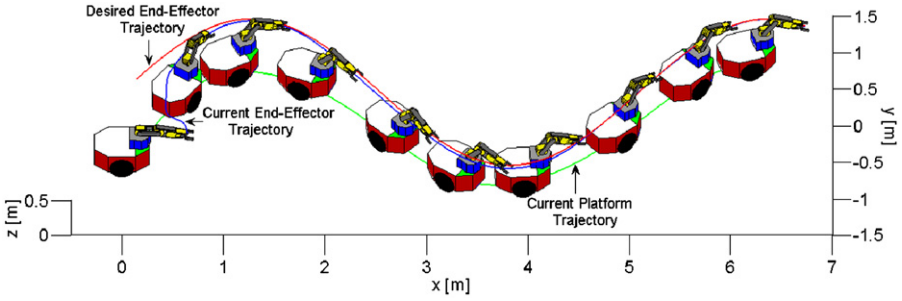

Fig. 14. Stroboscopic movement of the mobile manipulator in the trajectory tracking experiment.

A sufficient condition for $\dot{V}(\tilde{\mathbf{h}})$ to be negative definite is

$$\left|\tilde{\mathbf{h}}^{\mathbf{T}}\mathbf{L}_{\mathbf{K}}\tanh(\mathbf{L}_{\mathbf{K}}^{-1}\mathbf{K}\,\tilde{\mathbf{h}})\right| > \left|\tilde{\mathbf{h}}^{\mathbf{T}}(\mathbf{J}\tilde{\mathbf{v}}+\Upsilon)\right|. \tag{46}$$

Following a similar analysis to the one in Section 4.1, it can be concluded that, if

$$\|\mathbf{L}_{\mathbf{K}}\| > \frac{\|\mathbf{J}\tilde{\mathbf{v}}+\Upsilon\|}{\tanh(k_{aux})} \tag{47}$$

the position errors of the end-effector will be bounded by

$$\|\tilde{\mathbf{h}}\| \le \frac{k_{aux}\|\mathbf{J}\tilde{\mathbf{v}}+\Upsilon\|}{\varsigma\lambda_{min}(\mathbf{K})\tanh(k_{aux})} \quad \text{with } 0<\varsigma<1 \tag{48}$$

As proved in *Theorem 2*, the velocity error $\tilde{\mathbf{v}}(t)$ is ultimately bounded. Then, it can be concluded that the control error is also ultimately bounded by (48). □

5. Experimental results

In order to illustrate the performance of the proposed controller, several experiments were carried out for point stabilization, trajectory tracking and path following control of a mobile manipulator. The most representative results are presented in this section. The 6 DOF experimental system used in the experiments is shown in Fig. 8, which is composed of a non-holonomic mobile platform PIONEER 3AT, a laser rangefinder mounted on it, and a robotic arm CYTON Alpha 7 DOF (only 3 DOF of the 6 available DOFs are used in the

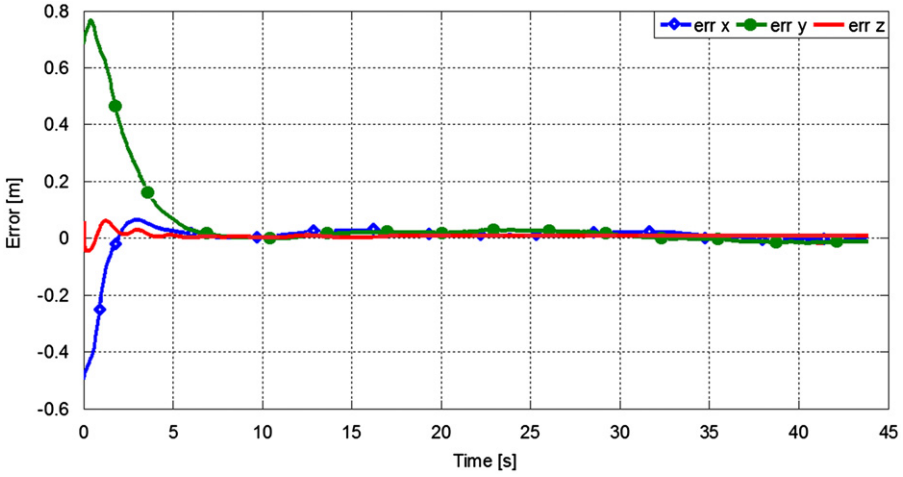

Fig. 15. Kinematic control errors $\tilde{\mathbf{h}}$ in the trajectory tracking experiment.

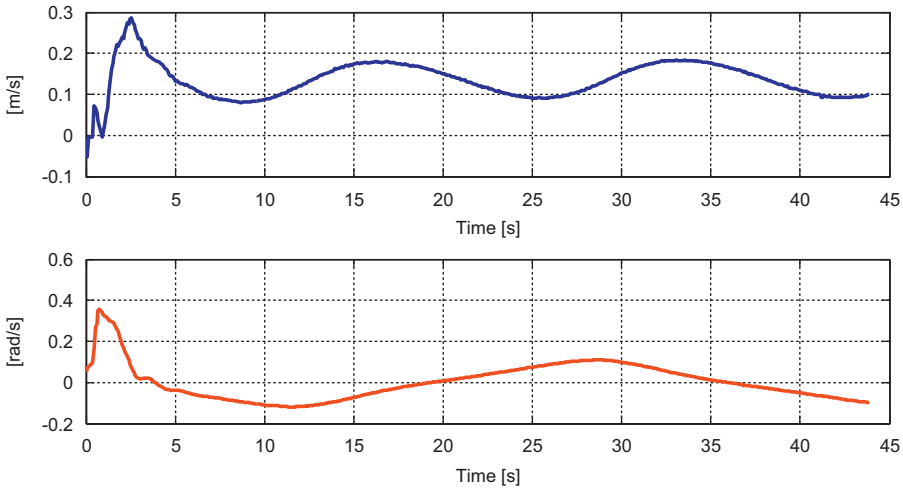

Fig. 16. Velocity commands to the mobile platform in the trajectory tracking experiment. Linear velocity command in the upper graph and angular velocity command in the lower graph.

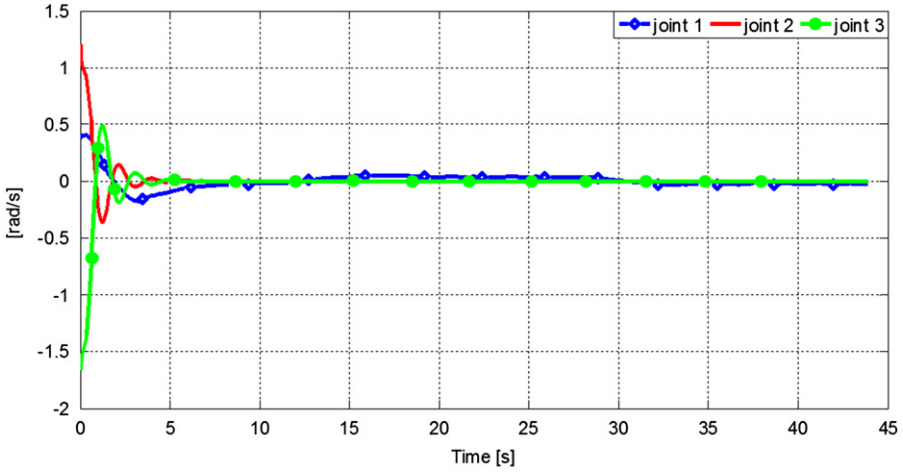

Fig. 17. Joint velocity commands for the robotic arm in the trajectory tracking experiment.

experiments). For the implementation of the experiments, internal sensors of the robot are used to calculate the control errors. Odometry sensor of the platform gives its position and orientation relative to a static framework, and arm's encoders give its joint displacements. Additionally, the laser range finder is used to detect obstacles in the path.

Dynamic compensation is performed for the mobile platform alone, because it presents the most significant dynamics of the whole mobile manipulator system.

For all experiments in this section it was considered that there is an error of 30% in model parameters. Also, the positions of the arm joints that maximize the arm's manipulability are obtained through numeric simulation. This way, the desired joint angles are $\theta_{1d} = 0$ rad, $\theta_{2d} = 0.6065$ rad, and $\theta_{3d} = -1.2346$ rad.

Four experiments are presented in order to evaluate the performance of the proposed scheme and to show the applicability of the unified algorithm to different motion control problems. The initial controller parameters will remain the same during all the experiments. The first experiment corresponds to the point stabilization control. In this experiment, the mobile platform starts at $q_p = \begin{bmatrix} 0\text{ m} & -0.5\text{ m} & 0\text{ rad} \end{bmatrix}^T$; the robotic arm at $q_a = \begin{bmatrix} 0\text{ rad} & 0\text{ rad} & 0\text{ rad} \end{bmatrix}^T$, and the desired final position of the

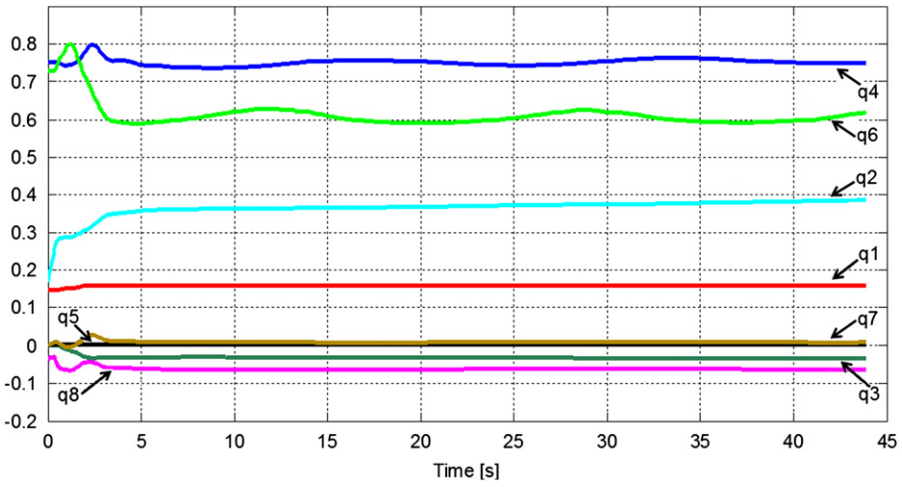

Fig. 18. Adaptive parameters evolution in the trajectory tracking experiment.

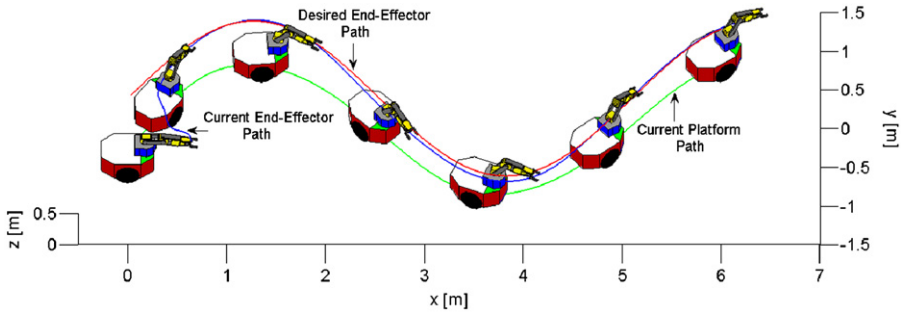

Fig. 19. Stroboscopic movement of the mobile manipulator in the path following experiment.

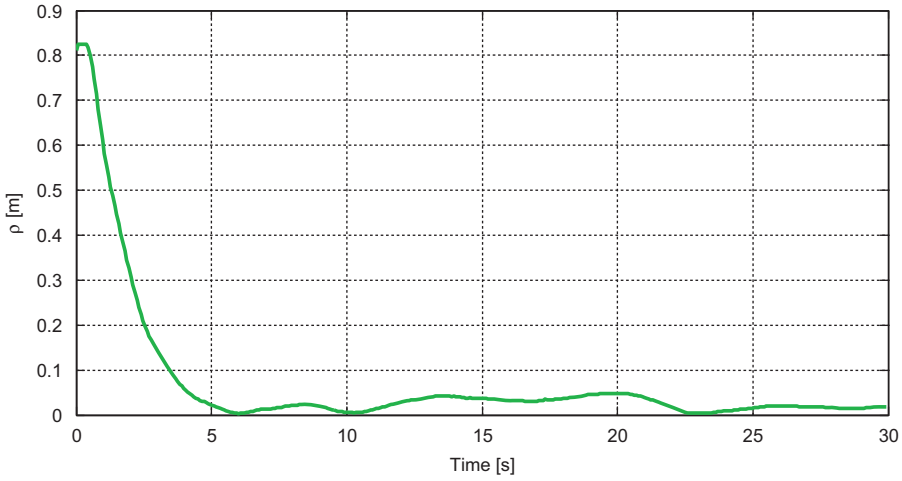

Fig. 20. Distance between the end-effector and the closest point on the path in the path following experiment.

end-effector is $\mathbf{h_d} = \begin{bmatrix} 3\text{m} & -2\text{m} & 0.55\text{m} \end{bmatrix}^{\text{T}}$. Additionally and only in this experiment, it is desired that the internal configuration of the mobile manipulator be $\theta_{1d} = \pi$ rad, $\theta_{2d} = 0.6065$ rad, and $\theta_{3d} = -1.2346$ rad. Matrix $\mathbf{H}$ used in the updating law is $\mathbf{H} = \text{diag}(33.4, 16.7)$. Also, controller's gains are set to $\mathbf{K} = \text{diag}(0.12,0.12,0.12)$; $\mathbf{L_K} = \text{diag}(0.15,0.15,0.15)$; $\mathbf{D} = \text{diag}(0.14, 0.2, 0.02, 0.02, 0.02)$; $\mathbf{L_D} = \text{diag}(0.7, 1.0, 0.1, 0.1, 0.1)$; $k_{vi} = 1$; $k_{uobs} = 0.5$; $k_{\omega obs} = 0.9$. And, maximum preset values for the control actions are 1 m/s for

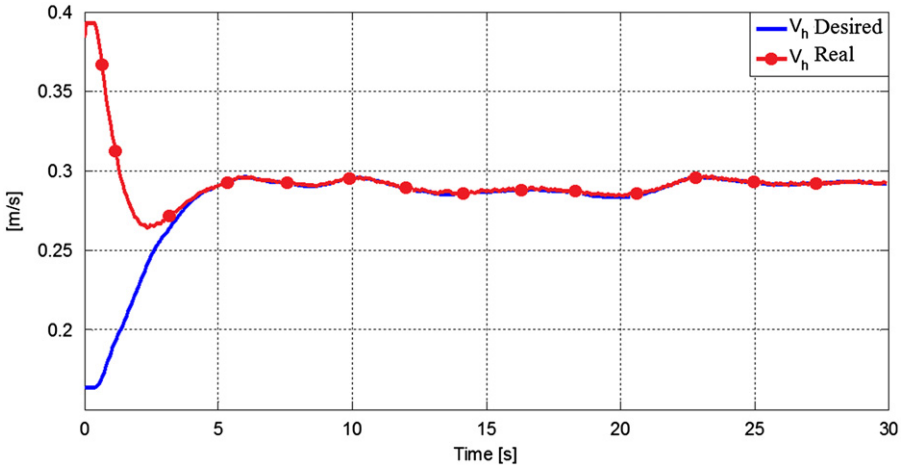

Fig. 21. Evolution of the desired and real end-effector velocities.

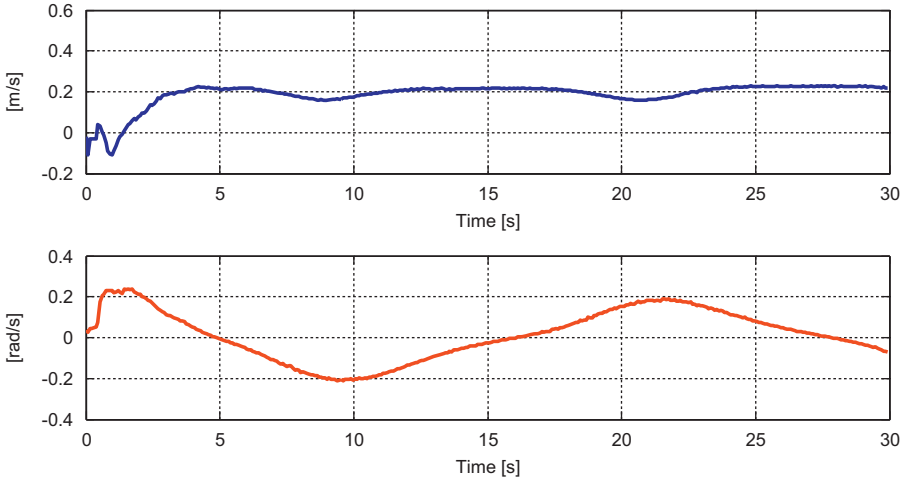

Fig. 22. Velocity commands to the mobile platform in the path following experiment. Linear velocity command in the upper graph and angular velocity command in the lower graph. Velocity commands to the mobile platform.

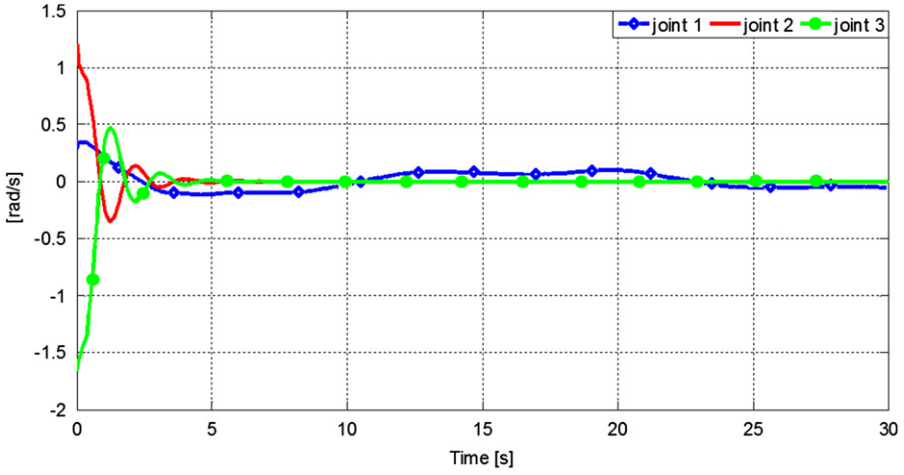

Fig. 23. Joint velocity commands for the robotic arm in the path following experiment.

the linear velocity, 2 rad/s for the angular velocity, and 1.5 rad/s for joint velocities.

Figs. 9–13 show the results of the first experiment. Fig. 9 shows the stroboscopic movement of the mobile manipulator. Fig. 10 shows that the control errors $\tilde{\mathbf{h}}(t)$ are ultimately bounded close to zero. Figs. 11 and 12 show the control actions of the robot, while Fig. 13 represents the evolution of the adaptive parameters, where it can be seen that all the parameters converge to fixed values.

The performance of the control algorithm for trajectory tracking will be tested in the second experiment. The desired trajectory for the end-effector is described by $\mathbf{h_d} = [x_{eed} \quad y_{eed} \quad z_{eed}]^T$, where

$$x_{eed} = 0.15t, \quad y_{eed} = \sin(\pi t/17), \quad z_{eed} = 0.47$$

It is important to mention that this trajectory was chosen in order to excite the dynamics of the mobile platform by changing its acceleration. Remember that, for trajectory tracking, $\mathbf{v_{hd}} \equiv \dot{\mathbf{h}}_\mathbf{d}$.

Figs. 14–18 represent the experimental results. Fig. 14 shows the desired trajectory and the current trajectory of the end-effector. It can be seen that the proposed controller presents a good performance. Fig. 15 shows the evolution of the tracking errors, which are ultimately bounded close to zero, while Figs. 16 and 17 show the control actions, which do not surpass the maximum preset values.

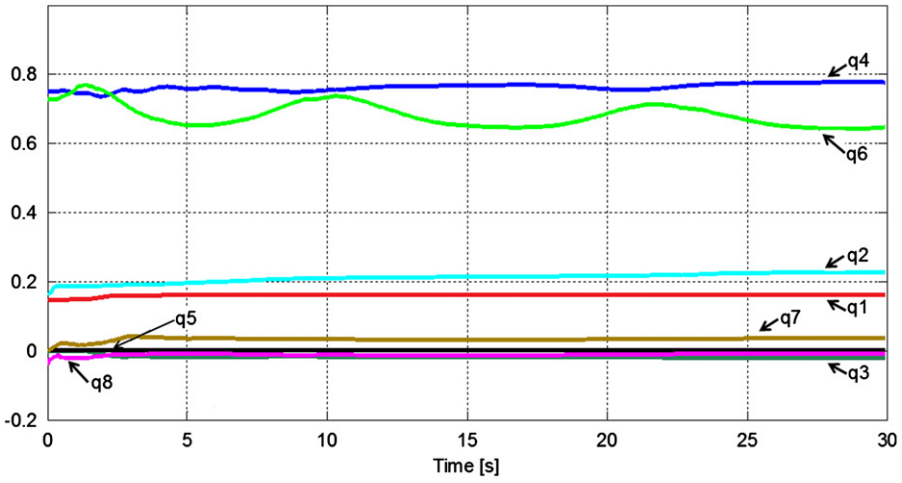

Fig. 24. Adaptive parameters evolution in the path following experiment.

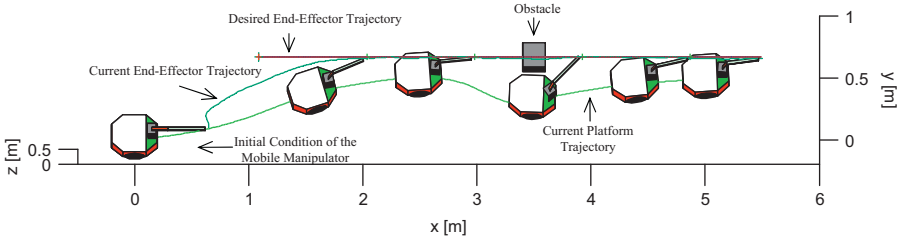

Fig. 25. Stroboscopic movement of the mobile manipulator in the trajectory tracking with obstacle avoidance experiment.

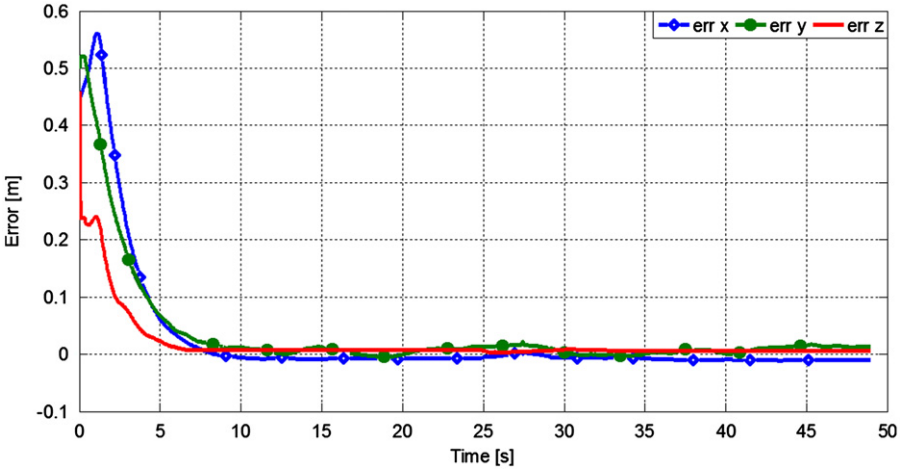

Fig. 26. Kinematic control errors $\tilde{\mathbf{h}}$ in the trajectory tracking with obstacle avoidance experiment.

Fig. 18 shows the evolution of the adaptive parameters; it can be seen that all the parameters converge to constant values.

Now, the next experiment corresponds to the path following control. In this experiment it is considered a similar path to the one corresponding to the second experiment. Note that for the path following problem, the desired velocity of the end-effector could depend on the task, the control error, the velocity of the mobile platform, the joint velocity of the arm, etc. In this experiment, it is considered that the reference velocity module depends on the desired velocity of the end-effector on the path P and on the control errors, as

$$|\mathbf{v_{hd}}| = \frac{\upsilon_P}{1+k_1|\tilde{\mathbf{h}}|}$$

where k_1 is a positive constant. Also, the desired location is defined as the closest point on the path to the end-effector of the experimental system.

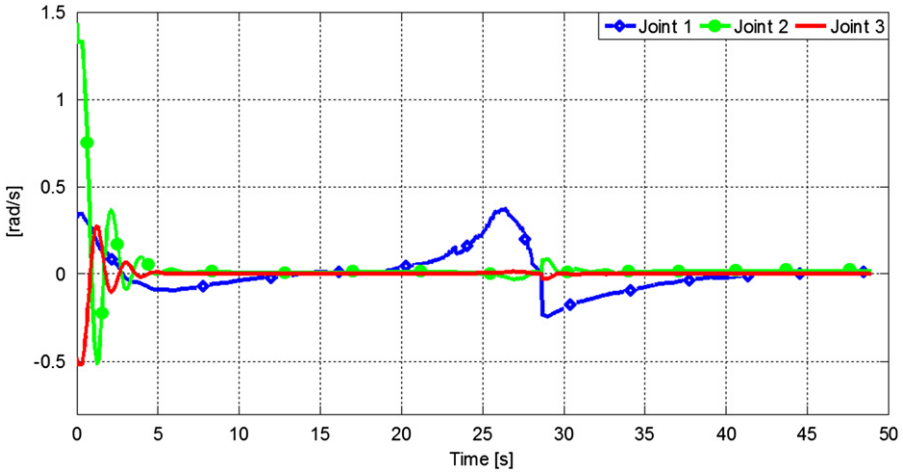

Fig. 27. Joint velocity commands for the robotic arm in the trajectory tracking with obstacle avoidance experiment.

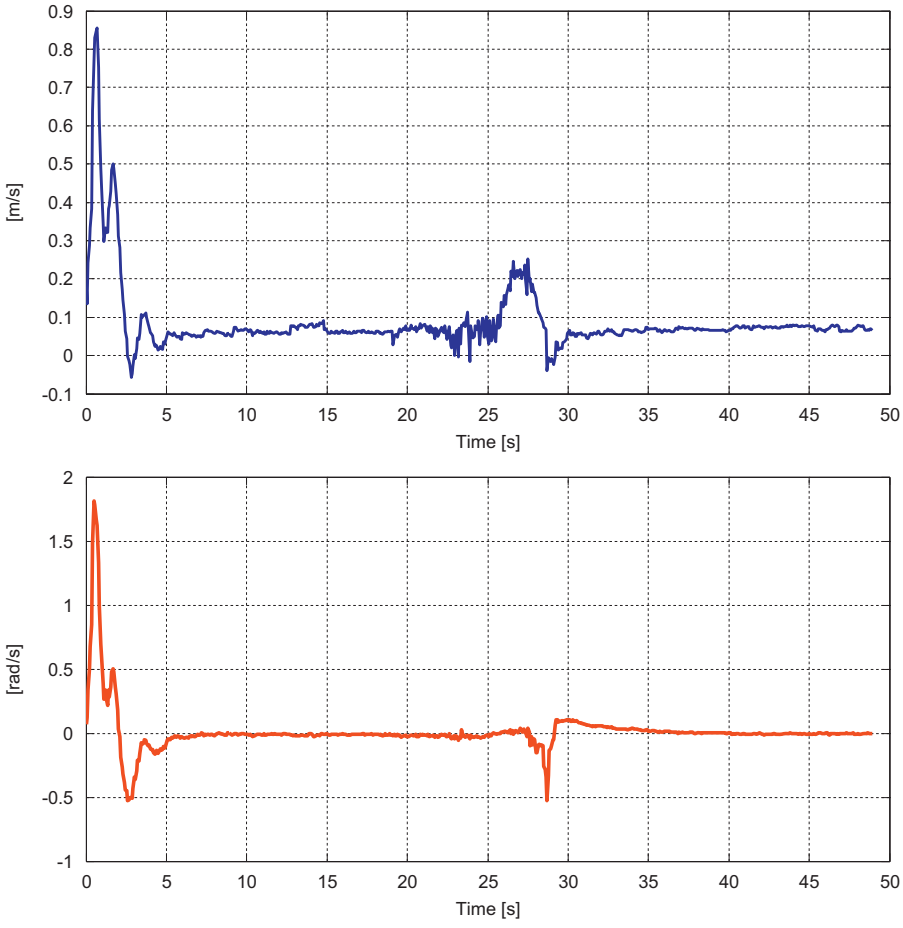

Fig. 28. Velocity commands to the mobile platform in the trajectory tracking with obstacle avoidance experiment. Linear velocity command in the upper graph and angular velocity command in the lower graph.

Fig. 19 shows the stroboscopic movement on the X–Y–Z space. It can be seen that the proposed controller works correctly. Fig. 20 shows that $\rho(t)$ is ultimately bounded close to zero. The evolution of the reference velocity and the actual velocity of the end-effector is illustrated in Fig. 21, where it can be seen that the reference velocity decreases in presence of large control errors. Figs. 22 and 23 show the control actions that do not surpass the maximum preset values of the robots, while Fig. 24 shows the evolution of the adaptive parameters which converge to fixed values.

Finally, it was planned to follow a spatial trajectory where an obstacle is placed so that the mobile platform can avoid it. It is considered that the obstacle is placed up to a maximum height that does not interfere with the manipulator arm; therefore the arm can follow the desired trajectory even when the platform is avoiding the obstacle.

Fig. 25 shows the stroboscopic movement on the X–Y–Z space. It can be seen that the proposed controller works correctly, both when tracking trajectories and when avoiding the obstacle. Fig. 26 shows that the tracking errors are ultimately bounded, while Figs. 27 and 28 show the control actions that do not surpass the maximum preset values.

6. Conclusions

In this paper a unified design of motion controllers for point stabilization, trajectory tracking and path following of a mobile manipulator has been presented . The design of the whole controller is based on two cascaded subsystems: a minimum norm kinematic controller which complies with the motion control objective, and an adaptive controller that compensates the dynamics of the mobile manipulator. Both, the kinematic controller and the adaptive controller have been designed to prevent from command saturation. Robot commands were defined in terms of reference velocities to the mobile platform and the manipulator joints. Stability and robustness are proved by Lyapunov's method. The performance of the proposed unified controller is shown through real experiments for the different motion control objectives: point stabilization, trajectory tracking and path following. Additionally, the obstacle avoidance functionality of the control algorithm is also experimentally evaluated. The experiments confirm the capability of the unified controller to solve different motion problems by an adequate selection of the control references. Also, the proposed control structure is general enough to admit any design for the dynamic compensation, which could include robust controllers that consider structural uncertainties or any other nonlinear dynamics.

Appendix A. Supplementary materials

Supplementary data associated with this article can be found in the online version at http://dx.doi.org/10.1016/j.conengprac.2012.07.008.

References

Andaluz, V., Roberti, F., & Carelli, R. (2010) Robust control with redundancy resolution and dynamic compensation for mobile manipulators. In *Proceedings of the IEEE international conference on industrial technology* (pp. 1469–1474). Viña del Mar, Chile, 14–17 March.

Bayle, B., & Fourquet, J. Y. (2001) Manipulability analysis for mobile manipulators. In *Proceedings of the IEEE international conference on robots & automation* (pp. 1251–1256). Seoul, Korea, 21–26 May.

Bayle, B., Fourquet, J. Y., & Renaud, M. (2003). Manipulability of wheeled mobile manipulators: Application to motion generation. *International Journal of Robotics Research*, *22*(7–8), 565–581.

Canudas de Wit, C., Siciliano, B., & Bastin, G. (1997). *Theory of robot control*. Great Britain: Springer-Verlag London Limited.

Chi-wu, B., & Ke-fei, X. (2009) Robust control of mobile manipulator service robot using torque compensation. In *Proceedings of the IEEE international conference on information technology and computer science* (pp. 69–72). Kiev, Ukraine, 25–26 July.

Chuyan, G., Zhang, M., & Sun, L. (2006). Motion planning and coordinated control for mobile manipulators. In *Proceedings of the 9th IEEE international conference on control, automation, robotics and vision* (pp. 1–6). Singapore, 5–8 December.

Das, Y., Russell, K., Kircanski, N., & Goldenberg, A. (1999). An articulated robotic scanner for mine detection—A novel approach to vehicle mounted systems. In *Proceedings of the SPIE conference: Detection and remediation technologies for mines and minelike targets IV* (pp. 5–9). Orlando, Florida, USA, 5–9 April.

De La Cruz, C., & Carelli, R. (2008). Dynamic model based formation control and obstacle avoidance of multi-robot systems. *Robotica*, *26*, 345–356.

De La Cruz, C., Freire Bastos, T., & Carelli, R. (2011). Adaptive motion control law of a robotic wheelchair. *Control Engineering Practice*, *19*(2), 113–125.

Dong, W. (2002). On trajectory and force tracking control of constrained mobile manipulators with parameter uncertainty. *Automatica*, *38*(9), 1475–1484.

Egerstedt, N., & Hu, X. M. (2000). Coordinated trajectory following for mobile manipulation. In *Proceedings of the IEEE international conference on robotics & automation* (pp. 3479–3484). San Francisco, CA, USA, 24–28 April.

Ge, W., Ye, D., Jiang, W., & Sun, X. (2008). Sliding mode control for trajectory tracking on mobile manipulators. In *Proceedings of the IEEE Asia Pacific conference on circuits and systems* (pp. 1834–1837). 30 November 30–3 December.

Gilioli, M., & Melchiorri, C. (2002). Coordinated mobile manipulator point-stabilization using visual-servoing techniques. In *Proceedings of the IEEE/RSJ international conference on intelligent robots and systems*. Lausanne, Switzerland, October 2002.

Hu Y. M., & Guo, B. H. (2004) Modeling and motion planning of a three-link wheeled mobile manipulator. In *Proceedings of the IEEE international conference on control, automation and vision* (pp. 993–998). Kunming, China, 6–9 December.

Kaufman, H., Barkana, I., & Sobel, K. (1998). *Direct adaptive control algorithms, theory and applications*. New York, USA: Springer.

Khatib, O. (1999). Mobile manipulation: The robotic assistant. *Robots Autonomous Systems*, *26*(2–3), 175–183.

Li, Z., Ge, S., Adams, M., & Wijesoma, W. (2008). Adaptive robust output-feedback motion/force control of electrically driven nonholonomic mobile manipulators. *IEEE Transactions on Control Systems Technology*, *16*(6), 1308–1315.

Li, Z., Yang, Y., & Li, J. (2010). Adaptive motion/force control of mobile under-actuated manipulators with dynamics uncertainties by dynamic coupling and output feedback. *IEEE Transactions on Control Systems Technology*, *18*(5), 1068–1079.

Liu, Y., & Li, Y. (2005). Sliding mode adaptive neural-network control for nonholonomic mobile modular manipulators. *Journal of Intelligent and Robotic Systems*, *44*(3), 203–224.

Mazur, A., & Szakiel, D. (2009). On path following control of nonholonomic mobile manipulators. *International Journal of Applied Mathematics and Computer Science*, *19*(4), 561–574.

Micaelli, A., & Samson, C. (1993). *Trajectory tracking for unicycle-type and two-steering-wheels mobile robots*. Technical Report No. 2097 of the Institut National De Recherche en Informatique et en Automatique Sophia-Antipolis. Available at: 〈http://hal.inria.fr/inria-00074575/en/〉 (accessed 01.02.11).

Monastero, A., & Fiorini, P. (2009). Target pose computation for non holonomic mobile manipulators. In: *Proceedings of the 14th IEEE international conference on advanced robotics*. Munich, Germany, 22–26 June.

Nasisi, O., & Carelli, R. (2003). Adaptive servo visual robot control. *Robotics and Autonomous Systems*, *43*(1), 51–78.

Paul, R. (1981). *Robot manipulators: Mathematics, programming, and control*. London, United Kingdom: MIT Press.

Phuong, N. T., Duy, V. H., Jeong, J. H., Kim, H. K., & Kim, S. B. (2007). Adaptive control for welding mobile manipulator with unknown dimensional parameters. In *Proceedings of the IEEE international conference on mechatronics* (pp. 1–6). Kumamoto, Japan, 8–10 May.

Sastry, S., & Bodson, M. (1989). *Adaptive control: stability, convergence and robustness*. Englewood Cliffs, New Jersey: Prentice-Hall.

Sciavicco, L., & Siciliano, B. (2000). *Modeling and control of robot manipulators*. Great Britain: Springer-Verlag London Limited.

Soeanto, D., Lapierre, L., & Pascoal, A. (2003). Adaptive non-singular path-following, control of dynamic wheeled robots. In *Proceedings of the 42nd IEEE conference on decision and control* (pp. 1765–1770). Hawaii, USA, 9–12 December.

Tsakiris, D. P., Kapellos, K., Samson, C., Rives, P., & Borrelly, J. J. (1997). Experiments in real time vision based point stabilization of a nonholonomic mobile manipulator. In *Proceedings of the fifth international symposium on experimental robotics*. Barcelona, Spain, June 15–18.

White, G., & Bhatt, M. (2009). Experimental evaluation of dynamic redundancy resolution in a non holonomic wheeled mobile manipulator. *IEEE/ASME Transactions on Mechatronics*, *14*(3), 349–357.

Wu, Y.X., Feng, Y., & Hu, Y. M. (2005). Dynamical adaptive sliding mode output tracking control of mobile manipulators. In *Proceedings of the 4th IEEE international conference on machine learning and cybernetics* (pp. 731–736). Guangzhou, China, 18–21 August.

Xu, D., Zhao, D., Yi, J., & Tan, X. (2009). Trajectory tracking control of omnidirectional wheeled mobile manipulators: Robust neural network-based sliding mode approach. *Proceedings of IEEE Transactions on Systems, Man, and Cybernetics—Part B: Cybernetics*, *39*(3), 788–799.

Yoshikawa, T. (1985). Manipulability of robotic mechanisms. *International Journal of Robotics Research*, *4*(2), 3–9.